Contents

List of Figures

List of Tables

Chapter 1

Introduction

1.1 Background

The n-body problem is a class of problems in physics that, in a highly general sense, consists of modelling the motion of n objects interacting through some physical force. In classical mechanics the equations of motion for n point particles can be derived from Newton's second law of motion, which states that the rate of change in momentum for an object equals the force acting on it, or from analytical formulations such as Lagrangian and Hamiltonian mechanics, which consider scalar properties of motion like kinetic and potential energies. In the quantum regime, where the wave-like property of matter has to be taken into account, the state of an n-body system is described by a total wave function, where the Hamiltonian operator generates the time evolution of the state as given by Schrödinger's differential equation.

The core of the n-body problem is that neither the classical equations of motion nor the Schrödinger equation are analytically solvable for more than two interacting particles. Consider the case where $n = 3$. Although apparently simple, the configuration space for the three-body problem is six dimensional after separating out the center of mass motion. Three additional constants of motion can be provided by conservation of the total angular momentum, which effectively reduces the problem to that of three coupled second order non-linear differential equations in the classical case and a three dimensional Schrödinger equation in the quantum case.

The quest for a general solution to the classical three-body problem is renowned. As a recurrent muse to a number of great mathematicians during the past centuries, dating back to Newton himself, the three-body problem has been a catalyst for the development of analysis and the modern theory of dynamical systems [5]. Although there are a number of special cases that have explicit solutions, non-linear dynamical systems often display highly unpredictable behaviour due to sensitive dependencies on initial conditions,

i.e. are chaotic. Nowadays, different numerical approaches are used to solve these kinds of problems, but the computational load can be substantial.

In contrast to the classical case, the quantum three-body problem is amenable to qualitative analysis [7] and in some cases, even to analytic solutions. In the quantum realm of few-body systems the Faddeev and the Faddeev-Yakubovsky equations, which are equivalent formulations of the Schrödinger equation for three- and four-body systems respectively, can, for a few special cases, be solved analytically by iteration [8, 23]. For the three-body scattering problem bound state solutions can exist in cases where all three two-body subsystems have short-ranged interactions, if at least two of these interactions are close to resonance. This is called the Efimov effect.

1.2 The Birth of Efimov Physics

In low energy scattering, particles are said to resonate when the strength of the attractive interaction between them barely cancels out the repulsive effect of the kinetic energy. During the collision they remain close for an extended period of time, in an almost bound state, before separating.

In 1970, Vitaly Efimov predicted that resonant two-body forces could give rise to a series of bound energy levels in three-particle systems [6]. When the short-ranged two-body forces approached resonance, he found a universal long-range three-body attraction emerging, giving rise to an infinite number of trimer states with binding energies obeying a discrete scaling law at resonance.

Efimov proposed that attractive three-body interaction appearing in systems with resonant short-ranged interactions and repulsive Coulomb forces could explain the binding of three particle nuclei such as the three nucleon triton ^{3}H and the triple-alpha Hoyle state of ^{12}C.

The notion of Efimov physics comprises a range of universal phenomena that occur in few-body systems exhibiting the Efimov effect. Short-ranged forces commonly occur in nature and few-body effects are expected to appear in a broad range of physical systems. Development in the theory of few-body quantum systems is important since it could bridge the gap between existing well developed models of treating one- and two-body systems and the statistical methods used to describe many-body systems.

1.3 Theoretical Introduction

A short reveiw concerning some important aspects of quantum mechanical systems and two-body scattering, in particlular the concept of *scattering length*, will follow in order to set the stage for a discussion of quantum effects in few-body systems in general and Efimov states in three-body systems in particular.

1.3.1 Entering the Quantum Realm

All particles of matter exhibit wave-like properties. The wavelength of a particle with momentum p is given by the de Broglie equation

$$\lambda = \frac{h}{p} = \frac{h}{mv} \tag{1.1}$$

where h is the Planck constant. The wave characteristics of matter grow with increasing de Broglie wavelength. When the wavelength is sufficently large, classical physics no longer applies and the system has reached the quantum regime. From 1.1 it is evident that this is true for particles that are very small or very slow. In an ultracold quantum gas, the atoms are cooled down to a point where they move so slowly that the increased uncertainty in position for the individual atoms becomes so large that they start to overlap with eachother. At this point the atoms cannot be viewed as individual particles but as a correlated wave. The de Broglie wavelength of the atoms is then larger than the average interatomic spacing, which is about one micron in a low density gas, and their behaviour are fully governed by quantum mechanics. In other words, the transition to the quantum regime occures when the thermal de Broglie wavelength is on the order of the interparticle spacing. Since the temperature of the gas and the thermal de Broglie wavelength are related through

$$\lambda = \frac{h}{\sqrt{2\pi m k_B T}}, \tag{1.2}$$

in which k_B is the Boltzmann constant, it means there is a critical temperature for when the quantum effects becomes dominant. For a dilute atomic gas this critical temperature are in the microkelvin to nanokelvin range.

1.3.2 Two-body Interactions

Atomic interactions are pair-wise and short ranged, which means that they interact when they are close to eachother. At sufficently low energies, atoms behave like point particles and have quantized orbital angular momenta l. In analogy with atomic orbitals, the quantum numbers $l = 0, 1, 2,$ associated with an atom are referred to as s-waves, p-waves, and d-waves respectively.

The scattering processes of two particles can be decomposed into that of an incoming plane wave – expanded into a sum of partial waves with definite angular momenta – which scatters of a potential placed at the origin. For low energy scattering, only the first few l-quantum numbers contribute to the scattering process and in the ultracold regime s-wave collisions dominate. Scattering becomes isotropic when the wavelength of the relative particle is much larger than the typical interparticle interaction range r_0 because the wave is then too large to resolve the details of the short-range interaction. In

other words, the colliding atoms cannot resolve each other's internal structure provided by their electron configurations. This makes scattering in the low energy limit indistinguishable from that of point particles. Furthermore, only spherical waves will come close enough to be scattered by the potential. Higher partial waves ($l > 0$) will not "feel" the potential since they will be reflected by a centrifugal barrier at separations greater then the interaction range. Two-body scattering in this regime are solely governed by a single parameter called the s-wave scattering length a. The s-wave scattering length, referred to as the scattering length from here on, is defined in the low-energy limit as

$$a = \lim_{k \to 0} -\frac{\tan \delta_0(k)}{k}, \tag{1.3}$$

where k is the wave number ($k = p/\hbar = \sqrt{2\mu E}/\hbar$) and $\delta_0(k)$ is the s-wave phase shift of the outgoing wave. For small k, the phase shift will behave as $\delta(k) \approx -ka + O(k^2)$. If scattering by a hard sphere is considered, the scattering length a is simply the radius of the sphere. In the low energy limit, the scattering properties for an arbitrary potential is the same as that of an hard sphere with radius a. Scattering can therefore occur at separations greater than the interaction range if the magnitude of the scattering length is sufficently large. The scattering length characterizes the strength of the short-range interparticle interaction. Since a positive scattering length correspond to a negative phase shift – which means the scattered wave is pushed out – the effective interaction will be repulsive and an increase in a will cause the underlying attractive potential in a two-body bound state to become less attractive. Increasing the magnitude of a negative scattering length will, on the other hand, make the potential more attractive since the phase shift is now positive and the scatterd wave is pulled in, see fig. 1.1. Even though the effective interaction is attractive at negative scattering lengths, the interaction will always be to weak to support a two-body bound state.

In the abscence of an interaction, the phase shift is simply zero. The strongest dephasing occurs when δ_0 takes the value $\pi/2$ (mod π), whereupon two-body s-wave resonances are formed. This situation is of particular interest in this theisis because Efimov physics arises when the two-body interactions are near resonance. Since the phase shift for the s-wave can be written as $\delta_0 \propto -ka$ in the long wavelength limit ($k \ll r_0^{-1}$), it means that the scattering length a has to become much larger in magnitude than the interaction range r_0 for a two-body interaction to become resonant.

1.3.3 Universality

Particles with large scattering lengths – i.e. $|a| \gg r_0$ – in the low-energy regime have universal properties. The properties are universal in the sense that they depend on the scattering length alone and not on the details of the

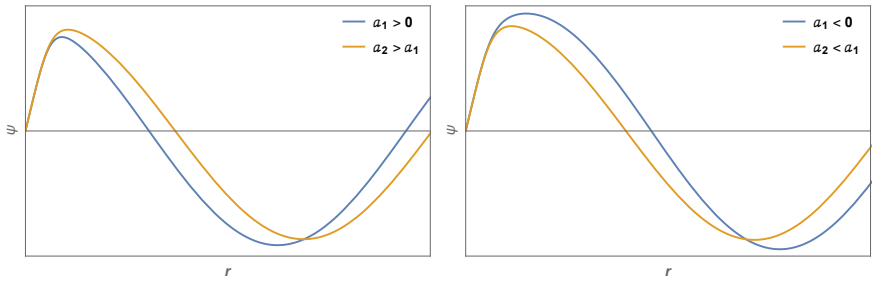

(a) The wave function is pushed outwards when the magnitude of a positive scattering length is increased.

(b) The wave is pulled inwards when the magnitude of a negative scattering length is increased.

Figure 1.1: Illustration of the phase shifts causing the effective interaction and how it depend of the sign and magnitude of a.

short-range interaction. For atoms interacting via short-ranged interactions the scattering length is considered large if its magnitude $|a|$ is much larger than the typical van der Waal length of the atomic species [4]. The van der Waal length is defined by

$$l_{vdW} = \left(\frac{2\mu C_6}{\hbar^2}\right)^{1/4}, \tag{1.4}$$

in which C_6 is the van der Waal coefficient of the r^{-6} term of the potental. For a system of two identical bosons with $a > 0$, there is a universal shallow two-body bound state near the scattering threshold, with binding energy

$$E_D = \frac{\hbar^2}{2\mu a^2}. \tag{1.5}$$

For $a < 0$ there is no such bound state. Outside the universal range the natural binding energy for two particles should be approximately $1/mr_0^2$. The cross section for elastic scattering of two identical bosons in this regime is also universal and so is the mean square radius, each given by

$$\sigma = 8\pi a^2 \tag{1.6}$$

and

$$\langle r^2 \rangle = \frac{a^2}{2}, \tag{1.7}$$

respectively. The universal quantities given in eqs. (1.5) to (1.7) are exact for $a = \pm\infty$ and approximate for $|a| \gg r_0$. The unique dependence on this one length parameter also leads to continuous scaling symmetries in these quantities. If the scattering length is scaled with some real factor λ such that $a \to \lambda a$, the shallow dimer energy will scale as

$$E_D(\lambda a) = \lambda^{-2} E_D(a), \tag{1.8}$$

while the elastic cross section and the mean square radius scale as

$$\sigma_e(\lambda^{-2}k, \lambda a) = \lambda^2 \sigma_e(k, a) \tag{1.9}$$

and

$$\langle r^2(\lambda a)\rangle = \lambda^2 \langle r^2(a)\rangle, \tag{1.10}$$

respectively.

While the scattering length completely governs the low energy two-body collision problem, it is also the main parameter for describing the interaction of particles at very low collision energies in general.

Similarly to the universal quantities found in the two-body sector, three-body systems can also exhibit universal properties. For particles interacting through short-ranged interactions near resonance – i.e. when the attraction are on the verge on, or can just bareley support a shallow dimer – an effective long-range three-body attraction emerge, which can form shallow three-body bound states with binding energies E_T^n that scale geometrically in the trimer region, see fig. 1.2. To understand how this long-range interaction is formed, consider a collision between the shallow dimer and a third particle in the low energy limit. The third particle will start to "feel" the dimer when it comes close to the two-body scattering length a, which is also the size of the dimer. At this point the third particle could tug off any of the particles in the dimer to form a new pair. It is this process of particle exchange which results in the effective three-body interaction that Vitaly Efimov found when he was studying the quantum three-body problem. This effective long-range attraction is universal in the sense that it emerges irrespective of the underlying two-body short-range interactions. The scaling in this sector is discrete. The infinite ladder of energy levels that appear in the asymptotic limit when $a \to \pm\infty$ have a discrete geometric scaling symmetry. The size of an excited state is larger than the previous state by a factor of $\lambda = e^{\pi/s_0} \simeq 22.7$. The scaling law applies radially see figure bla bla

$$\frac{E_T^{n+1}}{E_T^n} = e^{2\pi/s_0} \tag{1.11}$$

$$N \approx \pi^{-1} \ln(|a|/r_0) \tag{1.12}$$

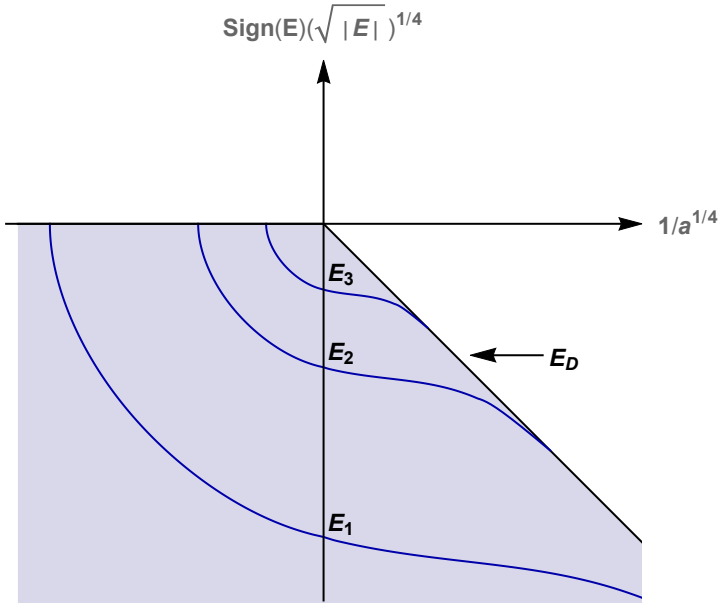

Figure 1.2: The energies of the three first Efimov states are plotted as a function of the inverse scattering length a. Three different regions can be identified in the figure. The three atom continuum is the region above the zero-energy threshold. The atom-dimer region is the region enclosed by the horisontal axis and the atom-dimer threshold and the trimer region shown in gray, in which Efimov states are represented by the blue lines.[3]

Chapter 2

Experimental Evidence

2.1 Efimov Trimers in Atomic Systems

Ultracold atomic clouds provided the first staging ground for exploring Efimov physics and related few-body phenomena because of the ability to control atom-atom interactions by an external field. In these extremely dilute gases, with densities n, the probability for collisions can reach unity by tuning the s-wave scattering length to the unitary regime $n|a^3| \gg 1$. In experiments with trapped ultracold atomic and molecular gases of alkali atoms with tunable two-body interactions, the existance of Efimov trimers have been inferred from resonantly enhanced loss rates, either in atomic three-body recombination processes at negative a, when the Efimov state couples to the triatomic threshold, or in atom-dimer relaxation processes.

Alkali atomic gases The first observations of an Efimov state was in an ultracold gas of ^{133}Cs was reported in 2006 by the group of Grimm and coworkers [14]. Later experiments have strengthen the evidence of these elusive states and in 2014 observations of the first exited Efimov state confirmed the theoretically predicted universal scaling properties of two succesive Efimov states [11]. Efimov resonances in homogenic gases with other atomic species have been observed including ^{85}Rb, ^{39}K, ^{7}Li, and three component fermi gases of ^{6}Li. Also mixtures mixtures of ^{41}K and ^{87}Rb has been investigated.

Helium trimers Helium is a prime candidate to study Efimov physics with a more direct approach. The ground state of the helium trimer is not an Efimov state. However the first and second exited trimer have Efimov characteristics. Coulomb explosion imaging of helium trimers have revealed the geometric form of the trimers. [15]

2.2 Efimov States in Nuclei

2.3 Four-body Recombination connected to Efimov Trimers

The Efimov scenario is even richer. In connection to an Efimov trimer, a pair of four-body states can form when a fourth atom approach. In accordance with the theoretical predictions, strong evidence for the existance of a pair of four-body states was provided in 2009 [9].

Chapter 3

Scattering Theory

3.1 Two-body Scattering

A collision between a pair of particles can be described in their center-of-mass frame as the scattering of a particle with reduced mass μ ($\mu = m_1 m_2/(m_1+m_2)$) by the potential $V(\mathbf{r})$. The time-independent Schrödinger equation for the relative motion is then given by

$$\left[-\frac{\hbar^2}{2\mu}\nabla^2 + V(\mathbf{r}) \right] \psi(\mathbf{r}) = \frac{\hbar^2 k^2}{2\mu}\psi(\mathbf{r}), \tag{3.1}$$

where $\mathbf{r}$ denotes the interparticle separation and ∇^2 the Laplace operator, which in spherical coordinates reads

$$\nabla^2 = \frac{1}{r^2}\frac{\partial}{\partial r}\left(r^2 \frac{\partial}{\partial r} \right) + \frac{1}{r^2 \sin\theta}\frac{\partial}{\partial \theta}\left(\sin\theta \frac{\partial}{\partial \theta} \right) + \frac{1}{r^2 \sin^2\theta}\frac{\partial^2}{\partial \phi^2}. \tag{3.2}$$

By requiring the potential to be zero at large interparticle separation, the collision can be described as that of an incident plane wave with definite angular momentum that scatters off a potential placed at the origin. The potential will deflect some of the incident waves to form scattered waves, which at large distances will be diverging from a point source in the scattering region. Let r_0 denote the range of the action of the potential and let z denote the direction of the propagation of the incident plane wave. The boundary condition at large separations $r \gg r_0$ then imposes a solution of the following asymptotic form

$$\psi(\mathbf{r}) \xrightarrow{r\to\infty} e^{ikz} + f(k,\theta,\phi)\frac{e^{ikr}}{r}, \tag{3.3}$$

in which the total wave function is written as a superposition of the incident and scattered wave, with a scattering amplitude $f(k,\theta,\phi)$ that depends on the energy of the particle through k, the deflection angle θ between the

waves and the azimuthal angle ϕ about the z-axis. For spherically symmetric potentials, i.e. $V(\mathbf{r}) = V(r)$, the Schrödinger equation (3.1) is separable. The incident and scattered wave functions are then conveniently expanded on a basis set of eigenfunctions of $\mathbf{L}^2$ and L_z, where $\mathbf{L}$ is the relative orbital angular momentum operator. These eigenfunctions are the spherical harmonic functions $Y_l^m(\theta, \phi)$, which satisfy

$$\mathbf{L}^2 Y_l^m(\theta,\phi) \equiv -\frac{1}{\sin^2\theta}\left[\sin\theta\frac{\partial}{\partial\theta}\left(\sin\theta\frac{\partial}{\partial\theta}\right)+\frac{\partial^2}{\partial\phi^2}\right]Y_l^m(\theta,\phi) = l(l+1)Y_l^m(\theta,\phi). \tag{3.4}$$

The most general solution to (3.1) is then of the form

$$\psi(\mathbf{r}) = \sum_{l=0}^{\infty}\sum_{m=-l}^{l} C_{lm}\frac{u_l(r)}{r}Y_l^m(\theta,\phi). \tag{3.5}$$

The separability of $\psi(\mathbf{r})$ effectively reduces the problem to that of solving the radial equation

$$\left[-\frac{d^2}{dr^2}+\frac{l(l+1)}{r^2}+\frac{2\mu}{\hbar^2}V(r)-k^2\right]u_l(r) = 0. \tag{3.6}$$

By requiring the wave function to be finite everywhere it is implied that $u_l(r)$ must vanish at the origin. In the case where $V(r) = 0$, the solutions to the radial equation for positive energies have the form

$$u_l(r) \propto r j_l(kr), \tag{3.7}$$

where $j_l(kr)$ are the spherical Bessel functions. In the case of a non-zero potential the solutions need to be regular at the origin, while at large distances $r \gg r_0$ they have the form

$$u_l(r) = r(a_l j_l(kr) + b_l y_l(kr)), \tag{3.8}$$

where $y_l(kr)$ are the spherical Neumann functions. Asymptotically the solutions (3.8) behave like

$$u_l(r) \xrightarrow{r\to\infty} \frac{1}{k}\big(a_l\sin(kr - l\frac{\pi}{2}) - b_l\cos(kr - l\frac{\pi}{2})\big). \tag{3.9}$$

By defining the ratio of the coefficients as

$$\frac{b_l}{a_l} = -\tan\delta_l(k), \tag{3.10}$$

where $\delta_l(k)$ is an energy dependent phase shift, the normalized asymptotic radial solutions for a non-vanishing potential can be written

$$\begin{aligned} u_l(r) \xrightarrow{r\to\infty} & \frac{1}{k}\big(\sin(kr - l\frac{\pi}{2} + \delta_l(k))\big) \\ = & \frac{e^{-i\delta_l(k)}}{2ik}\big((-1)^{l+1}e^{-ikr} + e^{2i\delta_l(k)}e^{ikr}\big). \end{aligned} \tag{3.11}$$

Since the incident plane wave (3.3) is aligned with the z-axis, it is an eigenfunction of L_z with an eigenvalue $m = 0$. The plane wave expansion is thus independent of the azimuthal angle around the z-axis and can therefore be expressed as

$$e^{ikz} = \sum_{l=0}^{\infty}(2l+1)i^l j_l(kr)P_l(\cos\theta), \tag{3.12}$$

where $P_l(\cos\theta)$ are the Legendre polynomials. It is evident that this plane wave is a solution to (3.1) for $V(r) = 0$. Asymptotically the solutions (3.12) behave like

$$e^{ikz} \xrightarrow{r\to\infty} \frac{1}{2ikr}\sum_{l=0}^{\infty}(2l+1)P_l(\cos\theta)\big((-1)^{l+1}e^{-ikr} + e^{ikr}\big). \tag{3.13}$$

The incident plane wave can thus be resolved into that of incoming (e^{-ikr}) and outgoing (e^{ikr}) spherical waves with a relative phase of 0 for l with odd parity and π otherwise. Substituting (3.13) into (3.3) results in an asymptotic wave function of the form

$$\psi(\mathbf{r}) \xrightarrow{r\to\infty} \frac{1}{2ikr}\sum_{l=0}^{\infty}(2l+1)P_l(\cos\theta))\big((-1)^{l+1}e^{-ikr} + e^{ikr}\big) + f(k,\theta)\frac{e^{ikr}}{r}, \tag{3.14}$$

where the scattering amplitude $f(k,\theta,\phi) = f(k,\theta)$ because the scattering potential is spherically symmetric. Since the system is rotationally invariant about the z-axis, the scattered wave function must be azimuthally symmetric, i.e. have a magnetic quantum number $m = 0$, wherefore the general solution (3.5) becomes

$$\psi(\mathbf{r}) = \sum_{l=0}^{\infty} c_l \frac{u_l(r)}{r}P_l(\cos\theta), \tag{3.15}$$

in which c_l are unknown coefficients. The asymptotic behaviour of (3.15) is thus

$$\psi(\mathbf{r}) \xrightarrow{r\to\infty} \frac{1}{2ikr}\sum_{l=0}^{\infty} c_l P_l(\cos\theta)e^{-i\delta_l(k)}\big((-1)^{l+1}e^{-ikr} + e^{2i\delta_l(k)}e^{ikr}\big). \tag{3.16}$$

By comparing the asymptotic form of the incoming waves expressed in eqs. (3.14) and (3.16) it is evident that the coefficents $c_l = (2l+1)e^{i\delta_l(k)}$. The asymptotic scattered wave is thus

$$\psi(\mathbf{r}) \xrightarrow{r\to\infty} \frac{1}{2ikr}\sum_{l=0}^{\infty}(2l+1)P_l(\cos\theta)\big((-1)^{l+1}e^{-ikr} + e^{2i\delta_l(k)}e^{ikr}\big). \quad (3.17)$$

For elastic scattering the flux of incoming and outgoing waves is conserved. The presence of a scattering potential will modify the plane wave by changing the relative phase of the incoming and outgoing waves by a phase shift $\delta_l(k)$ for each partial wave with angular momentum l. The phase shift $\delta_l(k)$ is thus a measure of the distortion of $u_l(r)$ from the free solution due to the presence of a scattering potential. Depending on whether the potential is attractive or repulsive, the scattered wave will either be pulled in or pushed out, respectively, by the scatterer. The scattering amplitude $f(k,\theta)$ is determined by comparing the outgoing waves in eqs. (3.14) and (3.17), resluting in

$$f(k,\theta) = \sum_{l=0}^{\infty}(2l+1)f_l(k)P_l(\cos\theta), \quad (3.18)$$

where the partial amplitude f_l can be expressed in the following ways

$$f_l(k) = \frac{e^{2i\delta_l(k)}-1}{2ik} = \frac{e^{i\delta_l(k)}\sin\delta_l(k)}{k} = \frac{1}{k\cot\delta_l(k) - ik}. \quad (3.19)$$

The differential and the total cross-sections are determined from the scattering amplitude through

$$\frac{d\sigma}{d\Omega} = |f(k,\theta)|^2, \quad (3.20)$$

and

$$\sigma(k) = \sum_{l=0}^{\infty}\sigma_l(k) = \frac{4\pi}{k^2}\sum_{l=0}^{\infty}(2l+1)\sin^2\delta_l(k), \quad (3.21)$$

in which σ_l is the scattering cross-section for each partial wave. So far, we have assumed that the particles are distinguishable and that scattering in the direction θ could be discriminated from that of scattering in the direction $\pi - \theta$. However, for identical particles these collisional processes will lead to the same final state. Interchaning the spatial coordinates of the particles $\mathbf{r}_1 \leftrightarrow \mathbf{r}_2$ corresponds to replacing the relative position vector $\mathbf{r}$ by $-\mathbf{r}$, which in polar coordinates corresponds to replacing (r,θ,ϕ) by $(r,\pi-\theta,\phi+\pi)$. Thus, to accurately describe scattering of identical particles the quantum

statistics of the particles must be taken into account to assure that the wave function of the total system has the correct symmetry properties. The wave function given in (3.3) does not fulfill this requirement. Instead, the correct two-body wave function in the center-of-mass frame for indistinguishable particles is retreived by symmetrization (bosons, $\epsilon = 1$) or antisymmetrization (fermions, $\epsilon = -1$), leading to

$$\psi(\mathbf{r}) \xrightarrow{r\to\infty} \frac{e^{ikz} + \epsilon e^{-ikz}}{\sqrt{2}} + \frac{f(k,\theta) + \epsilon f(k,(\pi-\theta))}{\sqrt{2}} \frac{e^{ikr}}{r}. \tag{3.22}$$

In classical mechanics, the differential cross-sections for the two processes described above would simply add up. However, the quantum mechanical differential cross-section for indistinguishable particles is given by

$$\frac{d\sigma}{d\Omega} = |f(k,\theta) + \epsilon f(k,(\pi-\theta))|^2, \quad \text{for} \quad 0 \le \theta \le \frac{\pi}{2}, \tag{3.23}$$

where the sum of probability amplitudes is

$$f(k,\theta) \pm f(k,(\pi-\theta)) = \frac{1}{2ik} \sum_{l=0}^{\infty} \left[1 \pm (-1)^l\right](2l+1) P_l(\cos\theta)(e^{2i\delta_l(k)} - 1). \tag{3.24}$$

Note that the total cross-section is obtained by integrating over half of the solid angle $\Omega = 4\pi$ in the case of identical particles. The expression for the total cross-section for elastic scattering after integration is then

$$\sigma(k) = \frac{8\pi}{k^2} \sum_{l=0}^{\infty} (2l+1) \sin^2 \delta_l(k). \tag{3.25}$$

In the case of bosons (fermions), only even (odd) values of l will contribute to the total cross-section (3.25).

3.2 The Low Energy Limit

At very low energies – i.e. when the angular de Broglie wavelength $\lambda\!\!\!^{-} = 1/k$ is much larger than the interparticle interaction range $kr_0 \ll 1$ – higher partial waves become unimportant except for potentials that are strong enough to form $l \neq 0$ bound states near threshold ($E \simeq 0$). This can be understood classically by considering that particles with angular momentum l and energies much lower than the height of the centrifugal barrier – i.e. the angular momentum term in the effective potential $V_{eff} = V(r) + \hbar^2 l(+1)/2\mu r^2$ – will simply be reflected by the barrier and only the lowest partial wave $l = 0$ will be able to come close enough to be scattered by the potential $V(r)$. For short-ranged two-body interactions – i.e. potentials that fall off faster than

r^{-2} – the angular momentum term is the potential of longest range and will thus largely govern the threshold behaviour ($E = 0$) of the radial wave function. Since the potential and the k^2 term can be neglected in the radial equation (3.6) for separations larger than the interaction range $r \gg r_0$, the general solution $R_l = u_l/r$ at threshold is given by

$$R_l(E = 0) = c_1 r^l + c_2 r^{-(l+1)}. \tag{3.26}$$

By joining this solution to the asymptotic solution for $E > 0$, given in (3.11) one can show that

$$\tan \delta_l(k) \simeq \delta_l(k) = \frac{c_2}{c_1} \frac{k^{2l+1}}{(2l-1)!!(2l+1)!!} = (-a_l k)^{2l+1}, \tag{3.27}$$

in which a_l is the scattering length for the lth partial wave. The arguments above form the basis of the Wigner threshold law [17, 19], which states that at near thershold, the phase shift goes to zero like

$$\delta_l(k) \propto k^{2l+1} \pmod{\pi} \quad \text{when} \quad k \to 0. \tag{3.28}$$

The cross-section for that partial wave then approaches zero like

$$\sigma_{l\neq 0}(k) = \frac{8\pi}{k^2}(2l+1)\sin^2 \delta_l(k) \propto k^{4l} \quad \text{when} \quad k \to 0, \tag{3.29}$$

wherefore s-wave scattering is dominant for short-ranged potentials in the low energy limit. The only non-zero cross-section is that for the s-wave, which using (3.19), is given by

$$\sigma = \sigma_0 = 8\pi \lim_{k\to 0} \left| \frac{1}{k \cot \delta_0 - ik} \right|^2 = 8\pi a^2, \tag{3.30}$$

in the case of identical bosons ($\sigma = 4\pi a^2$ for distinguishable particles) and where a is the s-wave scattering length, previously defined in (1.3).

3.2.1 Zero-Energy Scattering

In the ultracold regime the energy is extremely low and $k \simeq 0$. The radial equation simplifies to

$$-\frac{d^2 u_l(r)}{dr^2} + \frac{2\mu}{\hbar^2} V(r) u_l(r) = 0 \tag{3.31}$$

The asymptotic solution for $l = 0$ ($u = u_0$) is then

$$u(r) \xrightarrow{r\to\infty} \frac{1}{k} \sin\left[k\Big(r + \frac{\delta_0}{k}\Big)\right] \xrightarrow{k\to 0} \text{constant}(r - a). \tag{3.32}$$

The logarithmic derivative is given by

$$\frac{u'(r)}{u(r)} \xrightarrow{r\to\infty} k\cot\left[k\Big(r+\frac{\delta_0}{k}\Big)\right] \xrightarrow{k\to 0} \frac{1}{r-a}. \tag{3.33}$$

In the limit $kr \ll 1$, the scattering length is obtained as

$$a = -\lim_{k\to 0}\frac{\tan\delta_0}{k} = \lim_{k,r\to 0,\infty}\left(r - \frac{u(r)}{u'(r)}\right). \tag{3.34}$$

From equation (3.32) it is evident that the scattering length is simply the radius at which the tangent to the radial wave intercepts the r-axis. This concept can be illustrated by using a short-ranged attractive model potential given by

$$V(r) = -\frac{c_w\left[1-\left(1+\frac{r^2}{r_c^2}\right)e^{-\frac{r^2}{r_c^2}}\right]}{r^6}, \tag{3.35}$$

in which r_c and c_w are tuning parameters for the distance to the nadir and the depth of the potential, respectively. The scattering length can be varied by fine-tuning the potential depth, see fig. 3.2. Starting with an attractive potential with negative scattering length, i.e. with a tangent intercept on the negative side, when increasing the potential depth, the magnitude of the scattering length will increase and as $a \to -\infty$ the radial wave function will become flat. A further increase in potential depth will cause a to change sign $a \to \infty$. The sign shift of a is associated with the forming of a bound state. After the change in sign, a further increase in depth will instead correspond to decreasing a since the radial wave function now crosses the r-axis on the positive side, with the intercept subsequently approaching the origin, see fig. 3.1. This behavior is then repeated in the same way until a new bound state is formed, see fig. 3.3.

Positive scattering lengths thus correspond to replusive effective interactions, which means that the interaction can appear replusive even in the case of an underlying attractive two-body interaction.

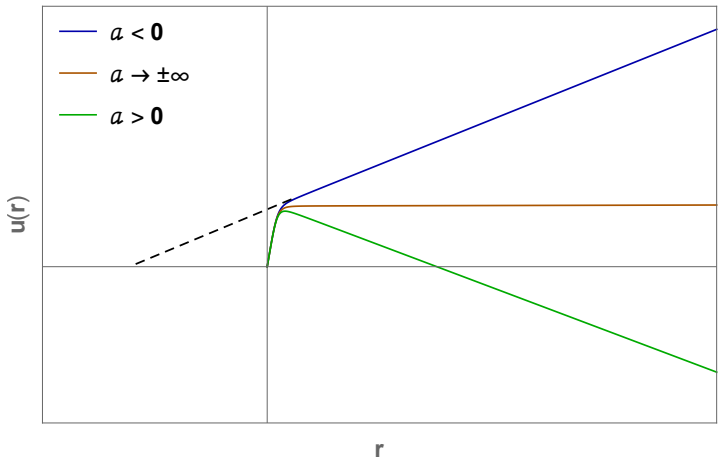

Figure 3.1: Plot of $u(r)$ versus r for the model potential (3.35) at three different depths. The radius at which the tangent intercept the r-axis gives the value of a.

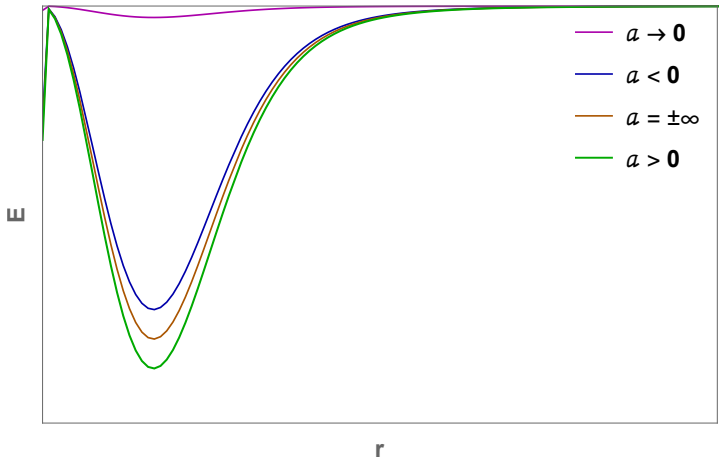

Figure 3.2: The three lowest curves correspond to the potentials used in fig. 3.1. As the magnitude of a negative a increases, the potential becomes more attractive until it reaches a constant depth at $a = \pm\infty$. After the change in sign, a further increase of a will instead have a repulsive effect on the interaction.

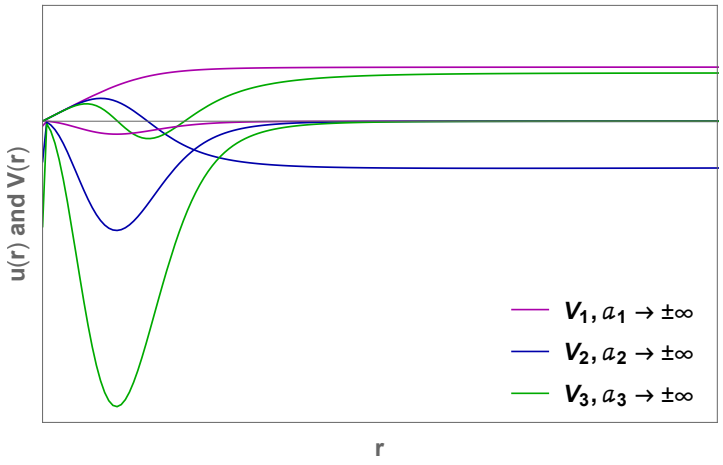

Figure 3.3: Illustration of three potentials and their coorsponding radial wave functions

Chapter 4

The Three-body Problem

Two-body scattering processes basically concern two different situations, elastic and inelastic collisions. For the three-body problem, solving the three-body Schrödinger equation is more involved. The enhanced complexity is mainly due to the increased number of fragmentation channels in the scattering processes. In addition to the triatomic fragmentation channel (1+1+1), there are three possible atom-dimer fragmenation channels (1+2). This makes the construction of permutation symmetric wavefunctions highly non-trivial.

There are different routes for solving the three-body problem and they involve either solving the three-body Schrödinger equation or solving the Faddeev equation, which is equivalent to solving the three-body Schrödinger equation in configuration space. Irrespective of the specific method of choice for solving the three-body system, most approaches start with the same steps. This includes separating out the center-of-mass motion and then defining a set of relative coordinates. A convenient choice for the three-body problem is mass normalized Jacobi coordinates, since this removes the mass factors in the kinetic energy operator.

Atomic units (a.u.) will be used throughout this theisis. There are four fundamental atomic units – the electron rest mass m_e, the elementary charge e, the reduced Planck's constant $\hbar$, and the Coulomb force constant k_e – which numerical values are unity by definition, i.e. $m_e = e = \hbar = k_e = 1$. Derived atomic units include dimensions of length and energy, which are expressed in terms of the Bohr radius a_0 and the Hartree E_h.

4.1 Mass Normalized Jacobi Coordinates

The spatial position of three particles in $\mathbb{R}^3$ are fixed by nine coordinates x_α^i, where $i(= 1, 2, 3)$ labels the particles, and $\alpha(= 1, 2, 3)$ their Cartesian space coordinates, respectively. Let $\mathbf{x}_i$ and m_i be the position vector and mass of the ith particle in the laboratory frame. If the total mass M, the

three particle reduced mass μ, and the normalizing constants d_k $(k = 1, 2, 3)$ are defined by

$$M = \sum_{i=1}^{3} m_i, \tag{4.1}$$

$$\mu^2 = \prod_{i=1}^{3} m_i/M, \tag{4.2}$$

$$d_k^2 = \frac{m_k}{\mu}\frac{(m_i + m_j)}{M}, \tag{4.3}$$

then a set of mass scaled Jacobi coordinates and the center-of-mass coordinate can be defined as

$$\mathbf{r}_k = d_k^{-1}(\mathbf{x}_j - \mathbf{x}_i), \tag{4.4}$$

$$\mathbf{R}_k = d_k\Big[\mathbf{x}_k - \frac{(m_i\mathbf{x}_i + m_j\mathbf{x}_j)}{m_i + m_j}\Big], \tag{4.5}$$

$$\mathbf{X}_{cm} = \frac{1}{M}\sum_{i=1}^{3} m_i\mathbf{x}_i, \tag{4.6}$$

in which the indices i, j, k are cyclic permutations of $(1, 2, 3)$ and where $\mathbf{r}_k$ is the scaled vector from particle i to j, and $\mathbf{R}_k$ is the scaled vector from the centre-of-mass of the pair ij to particle k, see fig. 4.1. The kinetic energy operator for the three particles in the laboratory frame, as given by

$$T = -\frac{1}{2}\sum_{i=1}^{3} m_i^{-1}\nabla_{\mathbf{x}_i}^2, \tag{4.7}$$

will subsequently transform into

$$T = -\frac{1}{2\mu}\Big(\nabla_{\mathbf{r}_k}^2 + \nabla_{\mathbf{R}_k}^2\Big) - \frac{1}{2M}\nabla_{\mathbf{X}_{cm}}^2. \tag{4.8}$$

Now, since the interaction $V(\mathbf{r}_k, \mathbf{R}_k)$ does not depend on $\mathbf{X}_{cm}$, the center-of-mass motion decouples from the internal motion in the Schrödinger equation if we write the wavefunction as

$$\Psi(\mathbf{r}_k, \mathbf{R}_k, \mathbf{X}_{cm}) = \varphi(\mathbf{X}_{cm})\psi(\mathbf{r}_k, \mathbf{R}_k), \tag{4.9}$$

so that

$$(H_{cm}+H_{int})\varphi_k(\mathbf{X}_{cm})\psi_n(\mathbf{r}_k, \mathbf{R}_k) = (E_k^{cm}+E_n^{int})\varphi_k(\mathbf{X}_{cm})\psi_n(\mathbf{r}_k, \mathbf{R}_k). \tag{4.10}$$

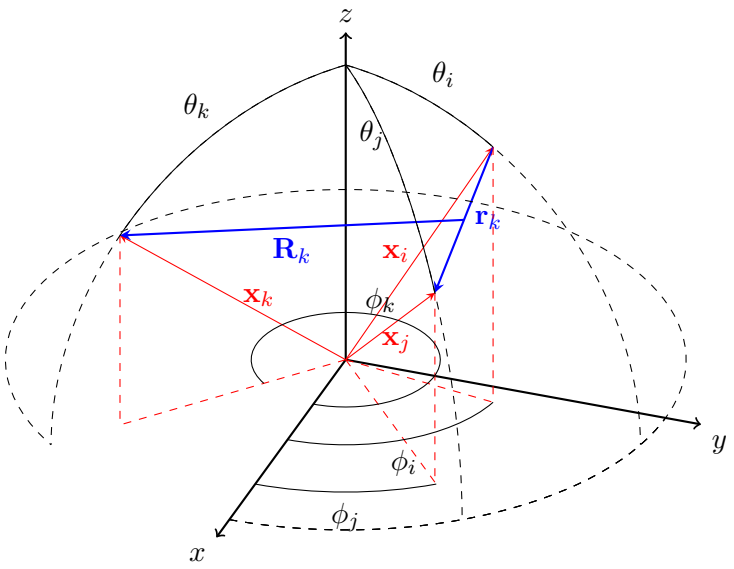

Figure 4.1: Spatial positions of three particles.

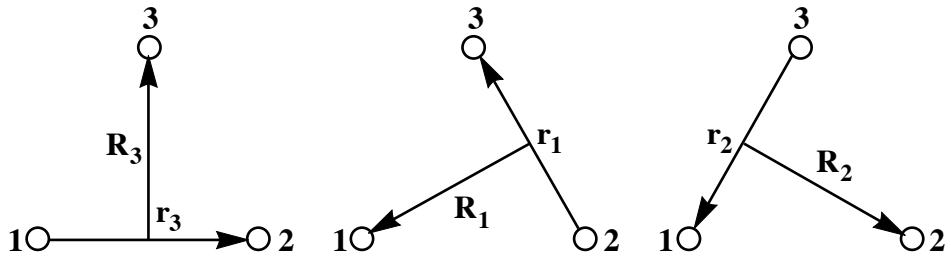

Figure 4.2: Illustration of the three different Jacobi coordinate sets.

Henceforth, we will only consider the internal motion part of the Schrödinger equation. To clarify the notations, from now on wavefunctions and energies labelled Ψ and E refers to the internal eigenstates and eigenenergies, which were labelled ψ and E^{int} previously.

There are three possible ways to construct the Jacobi coordinates described above, see Figure 4.2. Each set transforms into one of the other by exchange of particles. To be able to describe permutations in a system with mass-scaled coordinates it is useful to introduce angles defined by the particle masses [21]. If an even permutation (ijk) of the set (123) is considered, then the obtuse angle β_{ij} has the properties

$$\beta_{ij} = -\beta_{ji}, \quad \beta_{ii} = 0, \tag{4.11a}$$
$$\tan\beta_{ij} = -m_k/\mu, \tag{4.11b}$$
$$d_i d_j \sin\beta_{ij} = 1, \tag{4.11c}$$
$$d_i d_j m_k \cos\beta_{ij} = -\mu, \tag{4.11d}$$
$$\beta_{12} + \beta_{23} + \beta_{31} = 2\pi. \tag{4.11e}$$

Orthogonal transformations within the coordinate set are then given by

$$\begin{pmatrix} \mathbf{r}_j \\ \mathbf{R}_j \end{pmatrix} = \begin{pmatrix} \cos\beta_{ij} & \sin\beta_{ij} \\ -\sin\beta_{ij} & \cos\beta_{ij} \end{pmatrix} \begin{pmatrix} \mathbf{r}_i \\ \mathbf{R}_i \end{pmatrix}. \tag{4.12}$$

4.2 The Hyperspherical Method

The next common step in the theoretical framework to describe systems of three particles is to introduce hyperspherical coordinates. The components of the two vectors $\mathbf{r}$ and $\mathbf{R}$ are combined into a single, six-dimensional position vector $\mathbf{q}$. The components of this vector can be regarded as the cartesian components of a point in $\mathbb{R}^6$. The motion of a three particle system is thus equivalent to the motion of a single particle, with the reduced mass μ, in six-dimensional Euclidean space. The polar coordinates of this point particle are given by one hyperradial coordinate ρ, and five hyperangular coordinates, collectively labelled Ω. Three of these angles α, β, γ are usually chosen as the Euler angles that specify the orientation of the body-fixed axis system – i.e. the triangle formed by the three particles – relative to a space-fixed coordinate frame. These are the external coordinates of the system. The internal coordinates are the hyperradius – which describes the overall size of the system – and the remaining two hyperangles, which describe the shape of the triangle formed by the three particles.

Hyperspherical coordinates are useful for describing fragmentation problems. Fragmentation processes of the system into any one of the possible channels are described by the hyperradius becoming very large ($\rho \to \infty$), while the hyperangles distinguish between the different fragmentation channels. The hyperradius is invariant under both rotations and particle permutations, and for the three-body problem it is defined by

$$\rho = \left(\mathbf{r}^2 + \mathbf{R}^2\right)^{1/2}, \quad 0 \leq \rho < \infty. \tag{4.13}$$

In contrast to the hyperradius there is no unique way to define the hyperangles and the various definitions are not in general invariant under particle permutations. The most common choises of parametrizing the hypersphere fall into two distinct categories: Delves coordinates, and (democratic) Smith-Whitten coordinates.

Delves Coordinates

Delves coordinates are adapted to collinear atom-diatom collisions and are regular polar coordinates. They where originally developed to treat nuclear three-body problems. Each coordinate set is defined by the Jacobi vectors

$$r_k = \rho \sin \alpha_k, \tag{4.14}$$
$$R_k = \rho \cos \alpha_k, \tag{4.15}$$

where the Delves hyperangle α_k, which correlates to the lengths of these vectors, is defined by

$$\alpha_k = \arctan\left(\frac{r_k}{R_k}\right), \quad 0 \leq \alpha_k \leq \frac{\pi}{2}. \tag{4.16}$$

This coordinate set corresponds to the reactant arrangement when particle k scatters off the weakly bound particles ij. The other angle in this set is the angle between the two vectors $\mathbf{r}_k$ and $\mathbf{R}_k$. It is given by

$$\cos \theta_k = \frac{\mathbf{r}_k \cdot \mathbf{R}_k}{r_k R_k}, \quad 0 \leq \theta \leq \pi. \tag{4.17}$$

For simplicity, the indicies labelling each coordinate set will be surpressed from hereon.

The full derivation of the three-body Schrödinger equation written in Delves coordinates is given in appendix A, here we simply state the results. After rescaling the total wave function, $\psi = \rho^{5/2} \sin 2\alpha \Psi$, the Schrödinger equation can be written

$$\left(-\frac{1}{2\mu}\frac{\partial^2}{\partial \rho^2} + \frac{\Lambda^2 - 1/4}{2\mu\rho^2} + V(\rho, \alpha, \theta) \right) \psi(\rho, \alpha, \theta) = E\psi(\rho, \alpha, \theta), \tag{4.18}$$

in which E is the internal energy and where the squared grand angular momentum operator Λ^2, which contains all angular variables, is given by

$$\Lambda^2 = -\frac{\partial^2}{\partial \alpha^2} - \frac{1}{\sin^2 \alpha \cos^2 \alpha \sin \theta} \frac{\partial}{\partial \theta}\left(\sin \theta \frac{\partial}{\partial \theta} \right). \tag{4.19}$$

The corresponding volume element is proportional to $\rho^5 \sin^2 \alpha \cos^2 \alpha \sin \theta d\rho d\alpha d\theta$. To be square-integrable, the rescaled wavefunction for a bound state must obey the boundary conditions

$$\psi(0, \alpha, \theta) = 0, \tag{4.20}$$
$$\psi(\rho, 0, \theta) = \psi(\rho, \frac{\pi}{2}, \theta) = 0, \tag{4.21}$$
$$\left.\frac{\partial \psi}{\partial \theta}\right|_{\theta=0} = \left.\frac{\partial \psi}{\partial \theta}\right|_{\theta=\pi} = 0. \tag{4.22}$$

Numerical difficulties arise with these coordinates when permutation symmetries for three identical particles is considered [1].

Smith-Whitten Coordinates

The motion of three particles can be represented in a symmetric way by using so called democratic coordinates. The main advantage with these kind of coordinates is that permutation symmetries for three identical particles can be imposed exactly. To define the two hyperangles θ and ϕ we use the mapping procedure described by Johnson [12] to produce a modified set of the coordinates first introduced by Smith and Whitten [22]. The

$$\varphi_1 = 2\tan^{-1}(m_2/\mu) \tag{4.23}$$

$$\varphi_2 = 2\tan^{-1}(m_1/\mu) \tag{4.24}$$

Now we redefine $\phi'_k = \phi_k + 7\pi/2$, so that the range is $0 \leq \phi'_k < 4\pi$. Then $\sin\phi_k = \cos\phi'_k$. We finally get ($2\Phi = 4\pi - \phi'$)

$$r_3 = \frac{d_3\rho}{2^{1/2}}\left[1 + \sin\theta\cos\phi'\right]^{1/2} \tag{4.25}$$

$$r_1 = \frac{d_1\rho}{2^{1/2}}\left[1 + \sin\theta\cos(\phi' - \varphi_1)\right]^{1/2} \tag{4.26}$$

$$r_2 = \frac{d_1\rho}{2^{1/2}}\left[1 + \sin\theta\cos(\phi' + \varphi_2)\right]^{1/2}. \tag{4.27}$$

Now, we make a transformation of the angles (Kuppermann) and we get the final expression for the Hamiltonian

$$H = -\frac{\hbar^2}{2\mu}\left[-\frac{15}{4}\frac{1}{\rho^2} + \frac{\partial^2}{\partial\rho^2} + \frac{4}{\rho^2}\Big(\frac{1}{\sin(2\theta)}\frac{\partial}{\partial\theta}\sin(2\theta)\frac{\partial}{\partial\theta} + \frac{1}{\sin^2(\theta)}\frac{\partial^2}{\partial\phi^2}\Big)\right] + V(\rho,\theta,\phi) \tag{4.28}$$

$$= -\frac{\hbar^2}{2\mu\rho^2}\frac{\partial^2}{\partial\rho^2} + \frac{\hbar^2}{2\mu\rho^2}\left(\Lambda^2 + \frac{15}{4}\right) + V(\rho,\theta,\phi), \tag{4.29}$$

where Λ^2 is the grand angular momentum operator.

4.3 Adiabatic Hyperspherical Method

In the following sections we have chosen to work in the set of democratic hyperangles described in B. With these coordinates, the Schrödinger equation for the internal coordinates was derived as

$$\left(-\frac{1}{2\mu}\frac{\partial^2}{\partial\rho^2} + \frac{\Lambda^2+15/4}{2\mu\rho^2} + V(\rho,\theta,\phi)\right)\psi(\rho,\theta,\phi) = E\psi(\rho,\theta,\phi), \quad (4.30)$$

with boundary conditions

$$\frac{\partial\Phi_\nu(\rho;0,\phi)}{\partial\theta} = \frac{\partial\Phi_\nu(\rho;\frac{\pi}{2},\phi)}{\partial\theta}, \quad (4.31)$$

$$\frac{\partial\Phi_\nu(\rho;\theta,0)}{\partial\phi} = \frac{\partial\Phi_\nu(\rho;\theta,\frac{2\pi}{3})}{\partial\phi}, \quad (4.32)$$

reflecting three identical particle symmetry. We assume that the interactions V can be written as a sum of pairwise two-body potentials

$$V(\rho,\theta,\psi) = v(r_k) + v(r_i) + v(r_j). \quad (4.33)$$

The two-body interaction

$$v(r) = d\cosh^{-2}(r/r_0). \quad (4.34)$$

The general feature of the Efimov effect is that it is insensitive to the details of the interatomic interaction. Describe why it is okey to use model potentials, controlling the number of bound two-body systems, controlling the scattering length, tuning trough poles in the scattering matrix.

$$r_3 = 3^{-1/4}\rho[1+\sin\theta\cos\phi]^{1/2} \quad (4.35)$$

$$r_1 = 3^{-1/4}\rho[1+\sin\theta\cos(\phi-2\pi/3)]^{1/2} \quad (4.36)$$

$$r_2 = 3^{-1/4}\rho[1+\sin\theta\cos(\phi+2\pi/3)]^{1/2} \quad (4.37)$$

The exact solution to (4.30) can be found by first writing $\psi_n(\rho,\theta,\phi)$ as an expansion of radial wavefunctions $F_{\nu n}(\rho)$ and a set of complete, orthonormal channel functions $\Phi_\nu(\rho;\theta,\phi)$ that depend parametrically on ρ,

$$\psi_n(\rho,\theta,\phi) = \sum_{\nu=0}^{\infty} F_{n\nu}(\rho)\Phi_\nu(\rho;\theta,\phi). \quad (4.38)$$

The channel functions Φ_ν are solutions to the hyperangular part of (4.30)

$$\left(\frac{\Lambda^2+15/4}{2\mu_3\rho^2} + V(\rho,\theta,\phi)\right)\Phi_\nu(\rho;\theta,\phi) = U_\nu(\rho)\Phi_\nu(\rho;\theta,\phi), \quad (4.39)$$

and $U_\nu(\rho)$ are the resulting effective potental curves obtained by solving this eigenvalue equation at a number of different hyperradii. Substituting (4.38)

into (4.30) and projecting out $\Phi_{\nu'}$ by multiplying the conjugate transpose $\Phi_\nu^\dagger$ to the left and integrating over the hyperanglular coordinates results in an infinite set of coupled differential equation in ρ, which reads

$$\begin{aligned}&\Big(-\frac{1}{2\mu}\frac{\partial^2}{\partial\rho^2}+U_\mu(\rho)-\frac{1}{2\mu}Q_{\mu\mu}(\rho)\Big)F_{n\mu}(\rho)\\&-\frac{1}{2\mu}\Big(\sum_{\nu\neq\mu}2P_{\mu\nu}(\rho)\frac{\partial}{\partial\rho}+Q_{\mu\nu}(\rho)\Big)F_{n\nu}(\rho)=E_nF_{n\mu}(\rho),\end{aligned}\tag{4.40}$$

where the nonadiabatic coupling terms $P_{\mu\nu}$ and $Q_{\mu\nu}$ involve partial first and second derivative of the channel functions with respect to ρ. They are generated by the ρ dependence of the channel functions and are defined as

$$P_{\mu\nu}(\rho)=\Big\langle\!\Big\langle\Phi_\mu\Big|\frac{\partial}{\partial\rho}\Big|\Phi_\nu\Big\rangle\!\Big\rangle,\tag{4.41}$$

and

$$Q_{\mu\nu}(\rho)=\Big\langle\!\Big\langle\Phi_\mu\Big|\frac{\partial^2}{\partial\rho^2}\Big|\Phi_\nu\Big\rangle\!\Big\rangle,\tag{4.42}$$

where the double brackets denote integration over the two angular coordinates. Integration by parts, the completeness requirement of the channel-functions together with the antisymmetric properties of the coupling matrix $P_{\mu\nu}$, i.e. $P_{\mu\nu}=-P_{\nu\mu}$, are used to derive the following relation

$$Q_{\mu\nu}=\frac{dP_{\mu\nu}}{d\rho}+P_{\mu\nu}^2,\tag{4.43}$$

where the square of the coupling matrix $P_{\mu\nu}$ relates to $Q_{\mu\nu}$ through

$$\begin{aligned}P_{\mu\nu}^2&=\sum_\sigma P_{\mu\sigma}P_{\sigma\nu}=\sum_\sigma\Big\langle\!\Big\langle\Phi_\mu\Big|\frac{\partial\Phi_\sigma}{\partial\rho}\Big\rangle\!\Big\rangle\Big\langle\!\Big\langle\Phi_\sigma\Big|\frac{\partial\Phi_\nu}{\partial\rho}\Big\rangle\!\Big\rangle\\&=\sum_\sigma-\Big\langle\!\Big\langle\frac{\partial\Phi_\mu}{\partial\rho}\Big|\Phi_\sigma\Big\rangle\!\Big\rangle\Big\langle\!\Big\langle\Phi_\sigma\Big|\frac{\partial\Phi_\nu}{\partial\rho}\Big\rangle\!\Big\rangle=-\Big\langle\!\Big\langle\frac{\partial\Phi_\mu}{\partial\rho}\Big|\frac{\partial\Phi_\nu}{\partial\rho}\Big\rangle\!\Big\rangle.\end{aligned}\tag{4.44}$$

The antisymmetry of $P_{\mu\nu}$ together with $P_{\mu\nu}^2=P_{\nu\mu}^2$ leads to $P_{\nu\nu}=0$ and $Q_{\nu\nu}=P_{\nu\nu}^2$.

In the adiabatic hyperspherical approximation the diagonal elements are neglected and the effective potentials are defined as

$$W_\nu(\rho)=U_\nu(\rho)-\frac{1}{2\mu}Q_{\nu\nu}(\rho)=U_\nu(\rho)-\frac{1}{2\mu}P_{\nu\nu}^2(\rho).\tag{4.45}$$

The hyperspherical Born-Oppenheimer approximation, the effective potentials are simply $U_\nu(\rho)$, thus neglecting the diagonal terms.

$$W_\nu(\rho)=-\frac{s_0^2+1/4}{2\mu\rho^2}.\tag{4.46}$$

4.4 Generalized Hellmann-Feynman theorem

The following subsection concerns the mathematical description of the non-adiabatic coupling matrices that was defined in subsection 4.3. To obtain an expression for the coupling term $P_{\mu\nu}$ given in (4.41), a generalized Hellmann-Feynman (HF) approach can be used. Consider ν adiabatic eigenstates Φ_ν, which are obtained by

$$H_{ad}\Phi_\nu = U_\nu\Phi_\nu, \tag{4.47}$$

where the adiabatic Hamiltonian H_{ad} is just the hyperangular part of the Schrödinger equation given in (4.39), and the eigenvalues $U_\nu(\rho)$ are the effective adiabatic three-body potential curves. Using the identities

$$\Big\langle\!\Big\langle \Phi_\mu \Big| \Phi_\nu \Big\rangle\!\Big\rangle \equiv \delta_{\mu\nu} \tag{4.48}$$

and

$$\frac{\partial}{\partial\rho}\Big\langle\!\Big\langle \Phi_\nu \Big| \Phi_\nu \Big\rangle\!\Big\rangle \equiv 0, \tag{4.49}$$

we start by deriving the diagonal part of the HF theorem. Projecting Φ_ν out from equation (4.47), and differentiating with respect to the hyperradius gives

$$\begin{aligned}
\frac{\partial U_\nu}{\partial\rho} &= \frac{\partial}{\partial\rho}\Big\langle\!\Big\langle \Phi_\nu \Big| H_{ad} \Big| \Phi_\nu \Big\rangle\!\Big\rangle \\
&= \Big\langle\!\Big\langle \Phi_\nu \Big| \frac{\partial H_{ad}}{\partial\rho} \Big| \Phi_\nu \Big\rangle\!\Big\rangle + \Big\langle\!\Big\langle \Phi_\nu \Big| H_{ad} \Big| \frac{\partial\Phi_\nu}{\partial\rho} \Big\rangle\!\Big\rangle + \Big\langle\!\Big\langle \frac{\partial\Phi_\nu}{\partial\rho} \Big| H_{ad} \Big| \Phi_\nu \Big\rangle\!\Big\rangle \\
&= \Big\langle\!\Big\langle \Phi_\nu \Big| \frac{\partial H_{ad}}{\partial\rho} \Big| \Phi_\nu \Big\rangle\!\Big\rangle + U_\nu\Big\langle\!\Big\langle \Phi_\nu \Big| \frac{\partial\Phi_\nu}{\partial\rho} \Big\rangle\!\Big\rangle + U_\nu\Big\langle\!\Big\langle \frac{\partial\Phi_\nu}{\partial\rho} \Big| \Phi_\nu \Big\rangle\!\Big\rangle \\
&= \Big\langle\!\Big\langle \Phi_\nu \Big| \frac{\partial H_{ad}}{\partial\rho} \Big| \Phi_\nu \Big\rangle\!\Big\rangle + U_\nu\frac{\partial}{\partial\rho}\Big\langle\!\Big\langle \Phi_\nu \Big| \Phi_\nu \Big\rangle\!\Big\rangle \\
&= \Big\langle\!\Big\langle \Phi_\nu \Big| \frac{\partial H_{ad}}{\partial\rho} \Big| \Phi_\nu \Big\rangle\!\Big\rangle.
\end{aligned} \tag{4.50}$$

The generalized HF theorem also includes the nondiagonal terms. Multiplying with $\Phi_\mu^\dagger$ to the left of (4.47) and integrating over the two hyperangles, followed by differentiation with respect to the hyperradius gives

$$\begin{aligned}
&\frac{\partial U_\nu}{\partial\rho}\Big\langle\!\Big\langle \Phi_\mu \Big| \Phi_\nu \Big\rangle\!\Big\rangle + U_\nu\Big\langle\!\Big\langle \Phi_\mu \Big| \frac{\partial\Phi_\nu}{\partial\rho} \Big\rangle\!\Big\rangle + U_\nu\Big\langle\!\Big\langle \frac{\partial\Phi_\mu}{\partial\rho} \Big| \Phi_\nu \Big\rangle\!\Big\rangle \\
&= \Big\langle\!\Big\langle \Phi_\mu \Big| \frac{\partial H_{ad}}{\partial\rho} \Big| \Phi_\nu \Big\rangle\!\Big\rangle + U_\mu\Big\langle\!\Big\langle \Phi_\mu \Big| \frac{\partial\Phi_\nu}{\partial\rho} \Big\rangle\!\Big\rangle + U_\nu\Big\langle\!\Big\langle \frac{\partial\Phi_\mu}{\partial\rho} \Big| \Phi_\nu \Big\rangle\!\Big\rangle.
\end{aligned} \tag{4.51}$$

The first term on the left side of this equation i zero by the orthogonality of the channel functions. By removing the last term on both sides we obtain the final expression

$$\left\langle\!\left\langle \Phi_\mu \middle| \frac{\partial H_{ad}}{\partial \rho} \middle| \Phi_\nu \right\rangle\!\right\rangle = \big(U_\nu - U_\mu\big)\left\langle\!\left\langle \Phi_\mu \middle| \frac{\partial}{\partial \rho} \middle| \Phi_\nu \right\rangle\!\right\rangle, \tag{4.52}$$

and we can express the nonadiabatic coupling terms $P_{\mu\nu}$ as

$$P_{\mu\nu} = \frac{1}{\big(U_\nu - U_\mu\big)}\left\langle\!\left\langle \Phi_\mu \middle| \frac{\partial H_{ad}}{\partial \rho} \middle| \Phi_\nu \right\rangle\!\right\rangle. \tag{4.53}$$

Assume that the channel functions can be expressed as a series of basis functions

$$\Phi_\nu = \sum_j C_\nu^j \varphi_j, \tag{4.54}$$

Where C_ν^j are the expansion coeffients given in TODO(make reference). Anticipating that the Hamiltonian operator will take the matricial form of elements H_{ij}. From the results of the diagonal case discussed in, we obtain the following matrical expression [20]

$$\frac{\partial U_\nu}{\partial \rho} = \sum_{ij} (C_\nu^i)^\dagger C_\nu^j \frac{\partial H_{ij}}{\partial \rho}. \tag{4.55}$$

In the non-diagonal case the result in matrical form reads

$$\left\langle\!\left\langle \Phi_\mu \middle| \frac{\partial}{\partial \rho} \middle| \Phi_\nu \right\rangle\!\right\rangle = P_{\mu\nu} = \sum_{ij} (C_\mu^i)^\dagger C_\nu^j \frac{\partial H_{ij}}{\partial \rho}. \tag{4.56}$$

Chapter 5

Numerical Approach

In this thesis, the B-spline collocation method, with spatial discretization at Gauss points in each subinterval of the mesh with integration using Gauss-Legendre quadrature rule, is implemented to find the numerical solution of the adiabatic equation given in (4.39). The outline of this method is described in the following sections.

5.0.1 Basis splines expansion

The first step in solving the adiabatic equation, is to expand the solution, i.e. the channel functions Φ_ν, in a suitable basis, such as B-splines. The B-spline basis functions are piecewise polynomial functions which are defined using the *Cox-de Boor recursion formula*, see appendix C.

Basis functions in two dimensions can be generated from one-dimensional B-splines. If $\varphi_{1l},\ l = 1, \ldots, L$ is a basis for representing the functional dependency on θ and $\varphi_{2m},\ m = 1, \ldots, M$ is a basis for ϕ, then the tensor product basis is defined by

$$\varphi_{lm}(\theta, \phi) = \varphi_{1l}(\theta)\varphi_{2m}(\phi). \tag{5.1}$$

The two-dimensional basis can thus be built as a product of one-dimensional B-splines. The channel functions are then represented by

$$\Phi_\nu(\rho; \theta, \phi) = \sum_{l,m} c_{lm}\varphi_{lm}(\theta, \phi), \tag{5.2}$$

in which c_{lm} are LM unknown expansion coefficients. We then choose collocation at the knot points and require that (5.5) is a solution to (4.39) at those points. If we use B-splines of order k, defined as piecewise polynomials of order $(k-1)$ and define a mesh containing N_θ physical points in the θ-direction and N_ϕ physical points in the ϕ-direction, then we need to construct two knot point sequences, where k ghost points are put in the first and last physical point. The number of knot points in each grid are thus

$$\begin{aligned} P_\theta &= N_\theta + 2(k-1), \\ P_\theta &= N_\phi + 2(k-1). \end{aligned} \tag{5.3}$$

This means that the number of B-splines in each dimension are

$$\begin{aligned} L &= P_\theta - k = N_\theta + k - 2, \\ M &= P_\phi - k = N_\phi + k - 2. \end{aligned} \tag{5.4}$$

Thus we have LM B-splines and thus LM unknown coefficents but only $N_\theta N_\phi$ equations. Only $(k-1)^2$ B-splines are non-zero at the knot points, which means each equation involves $(k-1)^2$ B-splines

$$\Phi_\nu(\rho;\theta_i,\phi_j) = \sum_{l=i-k+1}^{i-1} \sum_{m=j-k+1}^{M} c_{lm}\varphi_{lm}(\theta_{j-1},\phi_{m+k-1}), \tag{5.5}$$

in which $(i = k,\ldots,j)$ The limits L and M can be reduced by placing boundary conditions on $\Phi_\nu(\rho;\theta,\phi)$. For each boundary condition on the coordinate in question, we get an additional equation and reduce the number of B-splines in that dimension by one. Thus, if $k = 6$ we need two boundary conditions for each dimension. The upper limits L and M are thus determined from

$$L = N_\theta + k - 2 - c_L, \tag{5.6}$$

$$M = N_\phi + k - 2 - c_M, \tag{5.7}$$

where $c_{L/M}$ denotes the number of boundary conditions for each coordinate. The number of unknowns are thus $(N_\theta + k - 2 - c_L)(N_\phi + k - 2 - c_M)$ and the number of equations are $(N_\theta + c_L)(N_\phi + c_M)$.

Boundary conditions are implemented by For a second order partial differential equation the B-splines must be twice differentiable everywhere on the knot sequence and have continuous second order derivatives. With the B-spline definitions given in C, the above requirements is fullfilled for B-splines of order $k \geq 4$. Next, substituting (5.5) into the adiabatic Hamiltonian (4.39) and projecting out $B_{l',k}(\theta)B_{m',k}(\phi))$ gives the matrix equation

$$\mathbf{Hc} = U\mathbf{Bc}, \tag{5.8}$$

where $\mathbf{c}$ is the column vector with the coefficients $c_\nu^{l,m}$. Mapping the two indices l and m into a single index i gives

$$i = (l-1)M + m. \tag{5.9}$$

The matrix elements of the Hamiltonian now reads

$$H_{i'i} = \iint d\theta d\phi B_{l',k}(\theta) B_{m',k}(\phi) H_{ad}(\rho;\theta,\phi) B_{l,k}(\theta) B_{m,k}(\phi), \tag{5.10}$$

and the overlap matrix elements are given by

$$B_{i'i} = \iint d\theta d\phi B_{l',k}(\theta) B_{m',k}(\phi) B_{l,k}(\theta) B_{m,k}(\phi). \tag{5.11}$$

The potential term in the adiabatic Hamiltonian cannot be separated into a product of two one-dimensional integral and must thus be integrated in two angular dimensions. Since the basis functions used in the expansion are B-splines, which are piecewise polynomial functions of degree $k-1$, the overlap matrix and the kinetic terms in the Hamiltonian can be evaluated exactly, within machine epsilon, using Gauss-Legendre quadrature.

5.0.2 Gauss-Legendre Quadrature

All integrals are calculated with Gaussian quadrature. A k-point Gaussian quadrature rule is constructed to give an exact result for polynomials of degree $2k-1$ or less by a suitable choice of the abscissas

$$\begin{aligned} &\int_{t_i}^{t_{i+1}} \int_{u_i}^{u_{i+1}} d\theta d\phi B_{l',k}(\theta) B_{m',k}(\phi) f(\theta,\phi) B_{l,k}(\theta) B_{m,k}(\phi) \\ &= \sum_{n=1}^{k} \sum_{p=1}^{k} w_n w_p B_{l',k}(\theta_n) B_{m',k}(\phi_p) f(\theta_n,\phi_p) B_{l,k}(\theta_n) B_{m,k}(\phi_p) \end{aligned} \tag{5.12}$$

Chapter 6

Results and Discussion

The results presented here concern the solution of the adiabatic equation. In order to obtain potential curves I solve Eq. (4.39) using a local function expansion such as the basis splines, thus determining the adiabatic potential curves U(R) 164 and the set of orthonormal channel functions (R; ,) that depend parametrically on R. In order to reach the assymptotic regime I have calculated The adiabatic equation (4.39) has been solved

N_θ	λ_{00}	λ_{13}	λ_{26}	array(s)	dsygvd(s)
5	0.000 000 000 0214	32.000 000 071 3015	60.000 002 031 0135	0.66	0.00
10	-0.000 000 000 0417	32.000 000 000 1003	60.000 000 000 2154	4.58	0.00
15	0.000 000 000 0007	32.000 000 000 1309	59.999 999 999 8871	12.32	0.02

Table 6.1: Numerically calculated eigenvalues

ρ (a.u.)	$N_\theta = 80$	$N_\theta = 100$
8000.0000	-0.99789324	-1.01719329
11666.667	-0.95232026	-0.94496812
15333.333	-0.59895416	-0.89254945
19000.000	0.74835108	-0.55523871
22666.667	2.18632828	0.58183597
26333.333	3.01480706	1.92849296
30000.000	3.42706459	2.81309001

Table 6.2: $a = -2702020$

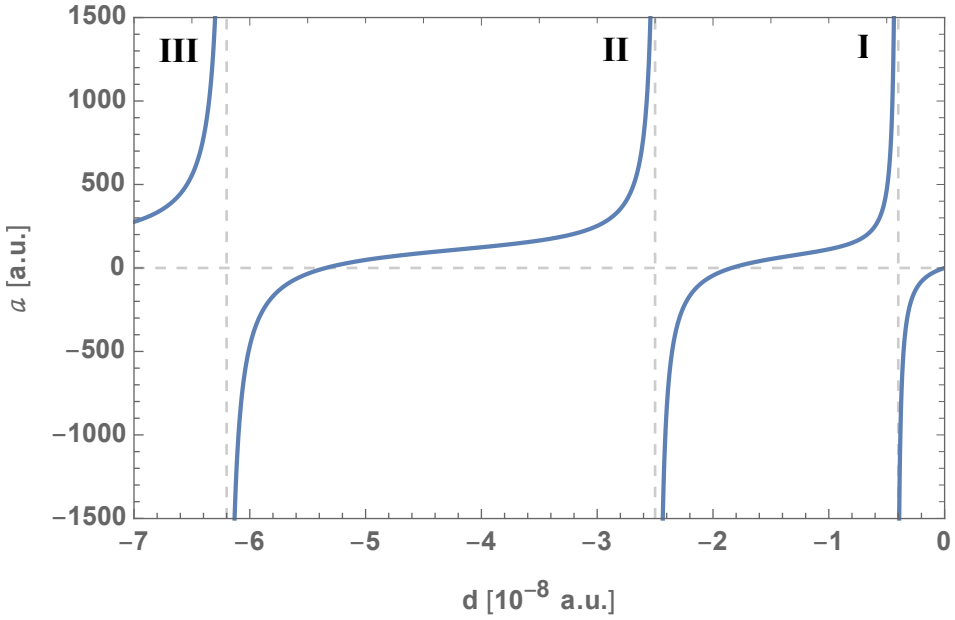

Figure 6.1: The two-body scattering length as a function of the potential depth d. Three poles can be recognized in the figure, labelled $\mathrm{I}, \mathrm{II}, \mathrm{III}$. At each pole a new two-body bound state is formed. The first bound state is formed as a passes through I, followed by a second a two-body bound state is formed. At each pole a new two-body bound state is formed, so when $|d|$ is increased so that a passes through II a second two-body bound state is formed, while a third state is formed as a passes through III.

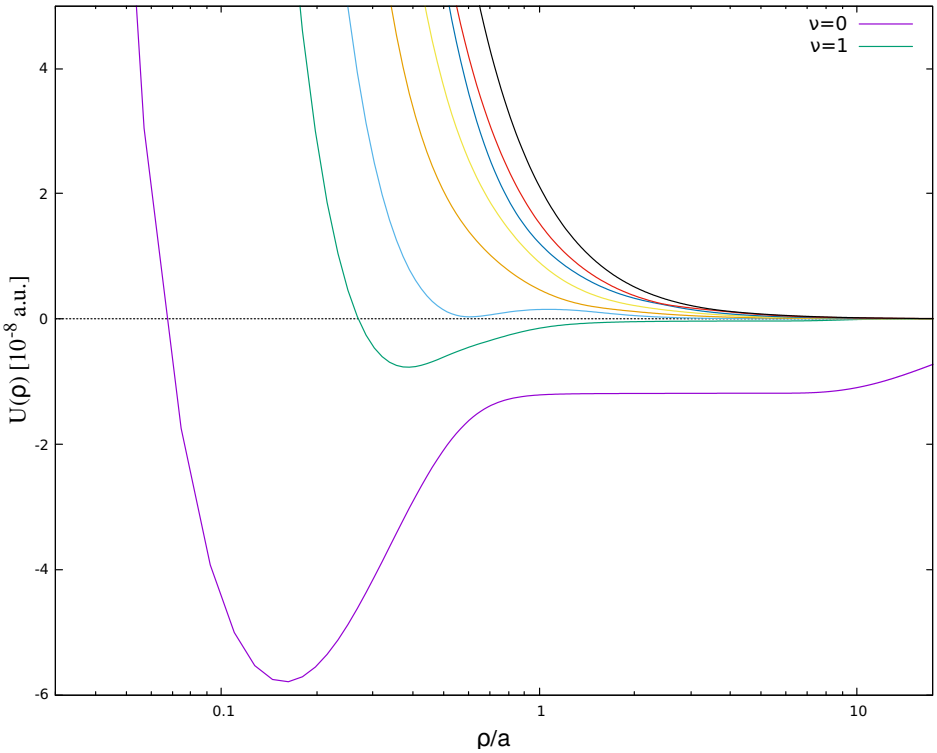

Figure 6.2: Adiabatic potential curves U_ν as a function of the hyperradius ρ for $a = 228$.

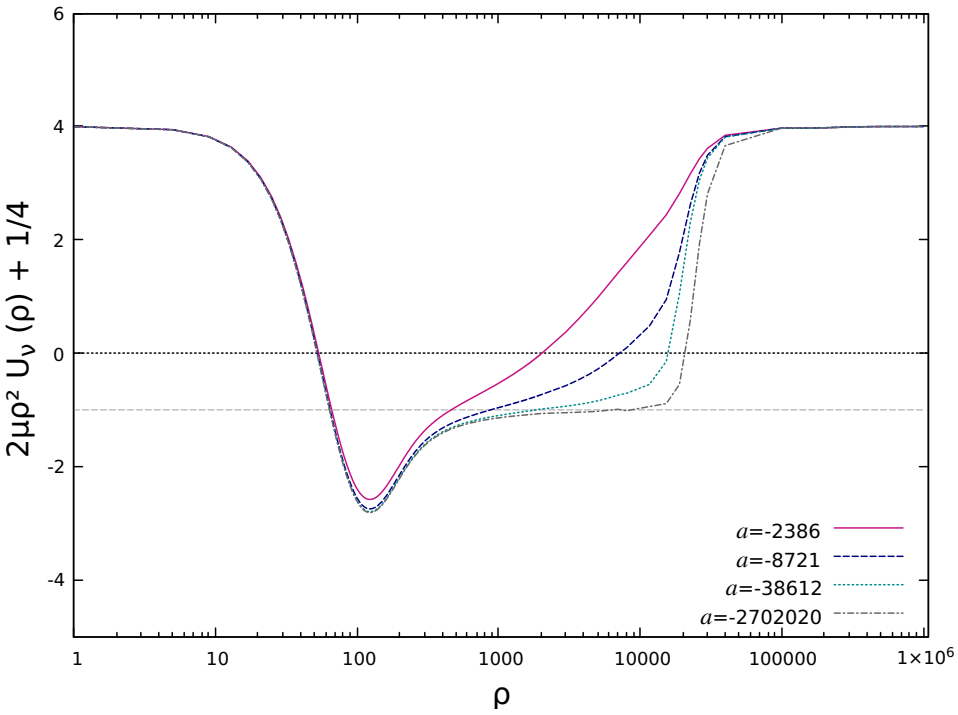

Figure 6.3: ..

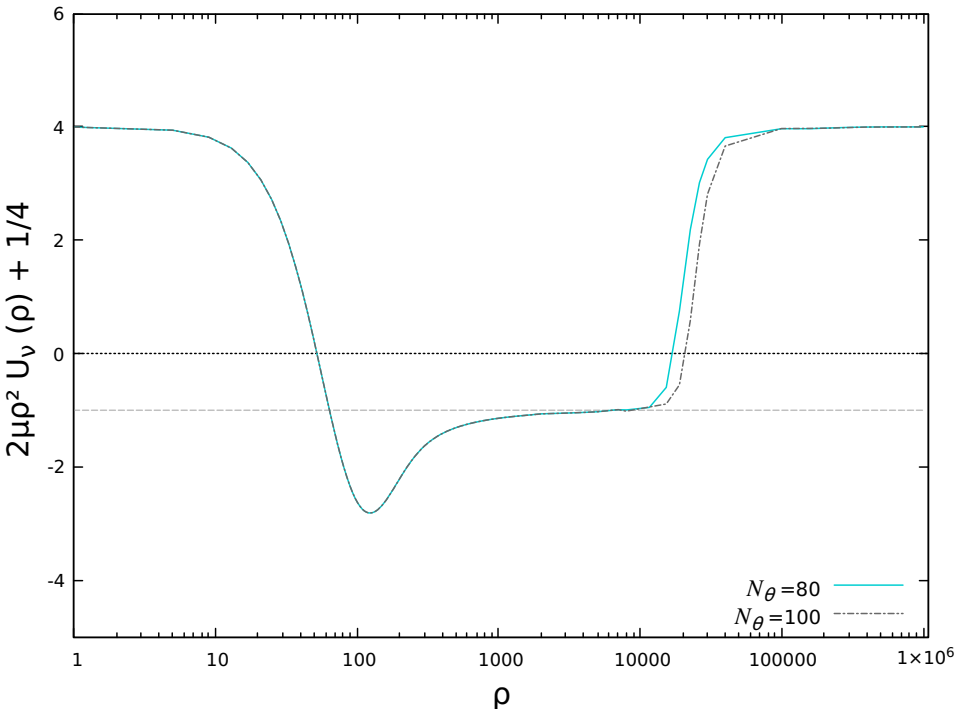

Figure 6.4: ..

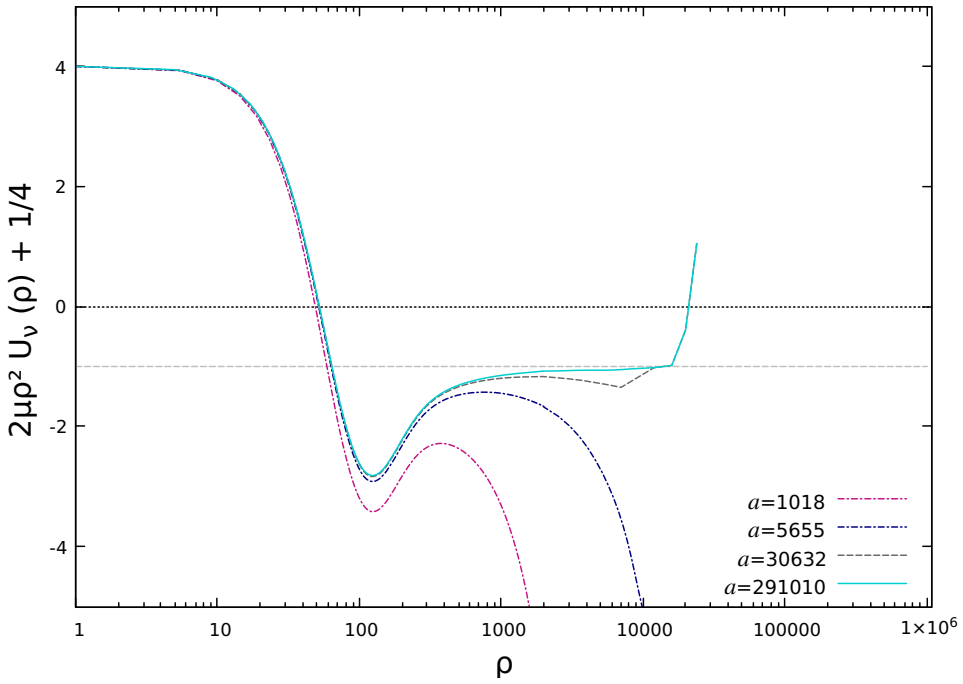
4
2
0
-2
-4
1
10
100
1000
10000
100000
1×10^6
ρ
2μρ² U_ν (ρ) + 1/4
a=1018
a=5655
a=30632
a=291010

Figure 6.5: ..

Appendix A

Delves Coordinates

This section contains the detailed derivation of the three-body Schrödinger equation written in Delves coordinates. The coordinate definitions are the same as in section 4.2. Here we simply repeat some previously stated definitions for a clearer overview. The Jacobi vectors in each coordinate set are defined by

$$r_k = \rho \sin \alpha_k, \tag{A.1a}$$
$$R_k = \rho \cos \alpha_k \tag{A.1b}$$

and the Delves hyperangle α_k is defined by

$$\alpha_k = \arctan\left(\frac{r_k}{R_k}\right), \quad 0 \leq \alpha_k \leq \frac{\pi}{2}. \tag{A.2}$$

The other angle in this coordinate set is the angle between the two vectors $\mathbf{r}_k$ and $\mathbf{R}_k$, which is given by

$$\cos\theta_k = \frac{\mathbf{r}_k \cdot \mathbf{R}_k}{r_k R_k}, \quad 0 \leq \theta \leq \pi. \tag{A.3}$$

The indices k will be suppressed from hereon. The mass weighted Schrödinger equation for the stationary wavefunction Ψ of a three-body system – with position vectors $\mathbf{x}_i$ and masses m_i, $(i = 1, 2, 3)$ – interacting pairwise through a potential V, is given by

$$-\frac{1}{2}\sum_{i=1}^{N} m_i^{-1} \nabla^2_{\mathbf{x}_i} \Psi + V\Psi = E\Psi. \tag{A.4}$$

Where ∇^2 is the Laplace operator, which in spherical coordinates reads

$$\Delta = \frac{1}{r^2}\frac{\partial}{\partial r}\left(r^2 \frac{\partial}{\partial r}\right) - \frac{L^2}{r^2}, \tag{A.5}$$

in which L is the angular momentum operator associated with the vector $\mathbf{r}$ and

$$L^2 = -\frac{1}{\sin\theta}\frac{\partial}{\partial\theta}\left(\sin\theta\frac{\partial}{\partial\theta}\right) - \frac{1}{\sin^2\theta}\frac{\partial^2}{\partial\phi^2}. \tag{A.6}$$

The kinetic energy for three particles in the mass normalized Jacobi coordinates was given in (4.8). Thus, after separating out the center-of-mass coordinate, the Schrödinger equation for the internal motion is simply

$$-\frac{1}{2\mu}\left(\nabla^2_{\mathbf{r}} + \nabla^2_{\mathbf{R}}\right)\Psi + V\Psi = E\Psi. \tag{A.7}$$

With the Laplacians for the mass scaled Jacobi vectors given by

$$\nabla^2_{\mathbf{r}} = \frac{1}{r^2}\frac{\partial}{\partial r}\left(r^2\frac{\partial}{\partial r}\right) - \frac{L_r^2}{r^2} = \frac{2}{r}\frac{\partial}{\partial r} + \frac{\partial^2}{\partial r^2} - \frac{L_r^2}{r^2}, \tag{A.8}$$

$$\nabla^2_{\mathbf{R}} = \frac{1}{R^2}\frac{\partial}{\partial R}\left(R^2\frac{\partial}{\partial R}\right) - \frac{L_R^2}{R^2} = \frac{2}{R}\frac{\partial}{\partial R} + \frac{\partial^2}{\partial R^2} - \frac{L_R^2}{R^2}. \tag{A.9}$$

If spin interactions are excluded the total orbital angular momentum is zero and we have

$$L_r^2 = L_R^2 = -\frac{1}{\sin\theta}\frac{\partial}{\partial\theta}\left(\sin\theta\frac{\partial}{\partial\theta}\right). \tag{A.10}$$

Change of coordinates subsequently results in the following transformations for the partial derivatives of the vector $\mathbf{r}$

$$\frac{\partial}{\partial r} = \frac{\partial\alpha}{\partial r}\frac{\partial}{\partial\alpha} + \frac{\partial\rho}{\partial r}\frac{\partial}{\partial\rho} = \frac{1}{\rho}\cos\alpha\frac{\partial}{\partial\alpha} + \sin\alpha\frac{\partial}{\partial\rho}, \tag{A.11}$$

$$\begin{aligned}\frac{\partial^2}{\partial r^2} &= \left(\frac{1}{\rho}\cos\alpha\frac{\partial}{\partial\alpha} + \sin\alpha\frac{\partial}{\partial\rho}\right)\left(\frac{1}{\rho}\cos\alpha\frac{\partial}{\partial\alpha} + \sin\alpha\frac{\partial}{\partial\rho}\right)\\ &= \frac{1}{\rho^2}\cos^2\alpha\frac{\partial^2}{\partial\alpha^2} - \frac{1}{\rho^2}\sin(2\alpha)\frac{\partial}{\partial\alpha} + \sin^2\alpha\frac{\partial^2}{\partial\rho^2}\\ &\quad + \frac{1}{\rho}\cos^2\alpha\frac{\partial}{\partial\rho} + \frac{1}{\rho}\sin(2\alpha)\frac{\partial^2}{\partial\alpha\partial\rho}.\end{aligned} \tag{A.12}$$

Similarly, the partial derivatives with respect to the vector $\mathbf{R}$ transform as

$$\frac{\partial}{\partial R} = \frac{\partial \alpha}{\partial R}\frac{\partial}{\partial \alpha} + \frac{\partial \rho}{\partial R}\frac{\partial}{\partial \rho} = -\frac{1}{\rho}\sin\alpha\frac{\partial}{\partial \alpha} + \cos\alpha\frac{\partial}{\partial \rho}, \tag{A.13}$$

$$\begin{aligned}\frac{\partial^2}{\partial R^2} &= \Big(-\frac{1}{\rho}\sin\alpha\frac{\partial}{\partial\alpha} + \cos\alpha\frac{\partial}{\partial\rho}\Big)\Big(-\sin\alpha\frac{\partial}{\partial\alpha} + \cos\alpha\frac{\partial}{\partial\rho}\Big) \\ &= \frac{1}{\rho^2}\sin^2\alpha\frac{\partial^2}{\partial\alpha^2} + \frac{1}{\rho^2}\sin(2\alpha)\frac{\partial}{\partial\alpha} + \cos^2\alpha\frac{\partial^2}{\partial\rho^2} \\ &+ \frac{1}{\rho}\sin^2\alpha\frac{\partial}{\partial\rho} - \frac{1}{\rho}\sin(2\alpha)\frac{\partial^2}{\partial\alpha\partial\rho}.\end{aligned} \tag{A.14}$$

Finally, the sum of the two Laplacian operators now reads

$$\begin{aligned}\nabla^2_{\mathbf{r}} + \nabla^2_{\mathbf{R}} &= \frac{2}{r}\frac{\partial}{\partial r} + \frac{2}{R}\frac{\partial}{\partial R} + \frac{\partial^2}{\partial r^2} + \frac{\partial^2}{\partial R^2} - \frac{L_r^2}{r^2} - \frac{L_R^2}{R^2} \\ &= \frac{4}{\rho^2}\cot(2\alpha)\frac{\partial}{\partial\alpha} + \frac{5}{\rho}\frac{\partial}{\partial\rho} + \frac{1}{\rho^2}\frac{\partial^2}{\partial\alpha^2} + \frac{\partial^2}{\partial\rho^2} \\ &+ \frac{4}{\rho^2\sin^2(2\alpha)\sin(\theta)}\frac{\partial}{\partial\theta}\Big(\sin(\theta)\frac{\partial}{\partial\theta}\Big) \\ &= \frac{1}{\rho^5}\frac{\partial}{\partial\rho}\Big(\rho^5\frac{\partial}{\partial\rho}\Big) + \frac{1}{\rho^2\sin^2(2\alpha)}\Big(\frac{\partial}{\partial\alpha}\sin^2(2\alpha)\frac{\partial}{\partial\alpha} + \frac{4}{\sin\theta}\frac{\partial}{\partial\theta}\Big).\end{aligned} \tag{A.15}$$

The original Hamiltonian operator written in Delves coordinates can thus be expressed as

$$H_0 = T_\rho + T_\alpha + T_\theta + V(\rho, \Omega). \tag{A.16}$$

Anticipating a rescaling of the wave function for subsequent removal of first derivatives with respect to ρ and α warrants us to write the kinetic energy operators in the original Hamiltonian in the following ways: Let the hyperradial kinetic energy operator T_ρ be expressed as

$$\begin{aligned}T_\rho &= -\frac{1}{2\mu}\Big[\frac{1}{\rho^5}\frac{\partial}{\partial\rho}\Big(\rho^5\frac{\partial}{\partial\rho}\Big)\Big] \\ &= -\frac{1}{2\mu}\Big[\rho^{-5/2}\Big(\rho^{5/2}\frac{5}{\rho}\frac{\partial}{\partial\rho} + \rho^{5/2}\frac{\partial^2}{\partial\rho^2}\Big)\rho^{-5/2}\rho^{5/2}\Big] \\ &= -\frac{1}{2\mu}\rho^{-5/2}\Big[-\frac{15}{4}\frac{1}{\rho^2} + \frac{\partial^2}{\partial\rho^2}\Big]\rho^{5/2}\end{aligned} \tag{A.17}$$

and let the kinetic energy operators for the hyperangles – that is, the kinetic energy operator for the Delves angle T_α and the kinetic energy operator for the angular momentum of the Jacobi vectors T_θ – be expressed as

$$
\begin{aligned}
T_\alpha &= -\frac{1}{2\mu}\frac{1}{\rho^2\sin^2(2\alpha)}\left[\frac{\partial}{\partial\alpha}\sin^2(2\alpha)\frac{\partial}{\partial\alpha}\right] \\
&= -\frac{1}{2\mu}\frac{1}{\rho^2}\left[\frac{\partial^2}{\partial\alpha^2} + 4\cot(2\alpha)\frac{\partial}{\partial\alpha}\right] \\
&= -\frac{1}{2\mu}\frac{1}{\rho^2}\left[\sin^{-1}(2\alpha)\left(\sin(2\alpha)\frac{\partial^2}{\partial\alpha^2} + 4\cos(2\alpha)\frac{\partial}{\partial\alpha}\right)\sin^{-1}(2\alpha)\sin(2\alpha)\right] \\
&= -\frac{1}{2\mu}\frac{1}{\rho^2}\sin^{-1}(2\alpha)\left[\frac{\partial^2}{\partial\alpha^2} + 4\right]\sin(2\alpha), \qquad \text{(A.18)}
\end{aligned}
$$

and

$$
\begin{aligned}
T_\theta &= -\frac{1}{2\mu}\left[\frac{4}{\rho^2\sin^2(2\alpha)\sin\theta}\frac{\partial}{\partial\theta}\left(\sin\theta\frac{\partial}{\partial\theta}\right)\right] \\
&= -\frac{1}{2\mu}\left[\frac{1}{\rho^2\sin^2\alpha\cos^2\alpha\sin\theta}\frac{\partial}{\partial\theta}\left(\sin\theta\frac{\partial}{\partial\theta}\right)\right] \qquad \text{(A.19)}
\end{aligned}
$$

respectively. Removal of first derivatives with respect to ρ and α is now possible by rescaling the total wave function such that $\Psi = \rho^{-5/2}(\sin(2\alpha))^{-1}\psi$. The corresponding transformation of the Hamiltonian is then

$$
\begin{aligned}
H &= \rho^{5/2}\sin(2\alpha)H_0\rho^{-5/2}(\sin(2\alpha))^{-1} \\
&= -\frac{1}{2\mu}\left[\frac{\partial^2}{\partial\rho^2} - \frac{15}{4\rho^2} + \frac{1}{\rho^2}\left(\frac{\partial^2}{\partial\alpha^2} + 4 + \frac{1}{\sin^2\alpha\cos^2\alpha\sin\theta}\frac{\partial}{\partial\theta}\left(\sin\theta\frac{\partial}{\partial\theta}\right)\right)\right] \\
&= -\frac{1}{2\mu}\left[\frac{\partial^2}{\partial\rho^2} + \frac{1}{\rho^2}\left(\frac{\partial^2}{\partial\alpha^2} + \frac{1}{\sin^2\alpha\cos^2\alpha\sin\theta}\frac{\partial}{\partial\theta}\left(\sin\theta\frac{\partial}{\partial\theta}\right)\right) + \frac{1}{4\rho^2}\right] \\
&= -\frac{1}{2\mu}\frac{\partial^2}{\partial\rho^2} + \frac{\Lambda^2 - 1/4}{2\mu\rho^2}, \qquad \text{(A.20)}
\end{aligned}
$$

where Λ^2 contains all the hyperangular kinetic energy variables. The squared grand angular momentum is in this case given by

$$
\Lambda^2 = -\frac{\partial^2}{\partial\alpha^2} - \frac{1}{\sin^2\alpha\cos^2\alpha\sin\theta}\frac{\partial}{\partial\theta}\left(\sin\theta\frac{\partial}{\partial\theta}\right). \qquad \text{(A.21)}
$$

The Schrödinger equation can thus be written

$$
\left(-\frac{1}{2\mu}\frac{\partial^2}{\partial\rho^2} + \frac{\Lambda^2 - 1/4}{2\mu\rho^2} + V(\rho,\alpha,\theta)\right)\psi(\rho,\alpha,\theta) = E\psi(\rho,\alpha,\theta), \qquad \text{(A.22)}
$$

where E is the internal energy. The corresponding volume element is proportional to $\rho^5\sin^2\alpha\cos^2\alpha\sin\theta d\rho d\alpha d\theta$. Since the rescaled wavefunction needs

to be square-integrable for a bound state, the boundary conditions are given by

$$\psi(0, \alpha, \theta) = 0, \tag{A.23}$$

$$\psi(\rho, 0, \theta) = \psi(\rho, \frac{\pi}{2}, \theta) = 0, \tag{A.24}$$

$$\left.\frac{\partial \psi}{\partial \theta}\right|_{\theta=0} = \left.\frac{\partial \psi}{\partial \theta}\right|_{\theta=\pi} = 0. \tag{A.25}$$

Appendix B

Smith-Whitten Coordinates

B.1 Coordinate Mapping

Johnson has given a detailed description of how the three-body system can be represented in a symmetric way [12]. In this section we present the main procedures used to retrieve a mapping for the three-dimensional triatomic potential energy surface to a point in configuration space. This mapping will treat the different arrangement channels equally, which enables permutation symmetries for three identical particles to be imposed exactly. Performing a second mapping of the original representation presented in [21, 22] yields the resulting set of modified Smith-Whitten coordinates. The derivation of the Hamiltonian for this representation is then described in appendix B.2. Some of the definitions presented in section 4.1 will be repeated here in oredr for this appendix to be complete.

Let $\mathbf{x}_i$ and m_i be the position vector and mass of the ith particle in the laboratory frame. If the total mass M, the three particle reduced mass μ, and the normalizing constants d_k $(k = 1, 2, 3)$ are given by

$$M = \sum_{i=1}^{3} m_i, \tag{B.1}$$

$$\mu^2 = \prod_{i=1}^{3} m_i/M, \tag{B.2}$$

$$d_k^2 = \frac{m_k}{\mu}\frac{(m_i + m_j)}{M}, \tag{B.3}$$

then the set of mass-scaled Jacobi vectors and the center of mass coordinate can be defined as

$$\mathbf{r}_k = d_k^{-1}(\mathbf{x}_j - \mathbf{x}_i), \tag{B.4}$$

$$\mathbf{R}_k = d_k\Big[\mathbf{x}_k - \frac{(m_i\mathbf{x}_i + m_j\mathbf{x}_j)}{m_i + m_j}\Big], \tag{B.5}$$

$$\mathbf{X}_{CM} = \frac{1}{M}\sum_{i=1}^{3} m_i\mathbf{x}_i, \tag{B.6}$$

in which, the indices i, j, k are cyclic permutations of $(1, 2, 3)$. The center-of-mass is separated out and will not be considered further. Transformations within the set of coordinates is aided by defining the angle β_{ij}, which have the following properties

$$\beta_{ij} = -\beta_{ji}, \quad \beta_{ii} = 0, \tag{B.7a}$$

$$\tan\beta_{ij} = -m_k/\mu, \tag{B.7b}$$

$$d_i d_j \sin\beta_{ij} = 1, \tag{B.7c}$$

$$d_i d_j m_k \cos\beta_{ij} = -\mu, \tag{B.7d}$$

$$\beta_{12} + \beta_{23} + \beta_{31} = 2\pi. \tag{B.7e}$$

Orthogonal transformations are then given by

$$\begin{pmatrix}\mathbf{r}_j\\ \mathbf{R}_j\end{pmatrix} = \begin{pmatrix}\cos\beta_{ij} & \sin\beta_{ij}\\ -\sin\beta_{ij} & \cos\beta_{ij}\end{pmatrix}\begin{pmatrix}\mathbf{r}_i\\ \mathbf{R}_i\end{pmatrix}. \tag{B.8}$$

To define a symmetric coordinate system, one starts by separating the external and internal coordinates of the configuration. For the external coordinates we use the Euler angles, these are used to relate rotations of the three-body system in space. Since the potential energy only depends on the internal coordinates we will focus on them here. The internal coordinates ρ, Θ, and Φ_k determine the size, shape and particle arrangement of the triangle formed by the three-body system, respectively. Starting from the definition for the internal coordinates given by Smith and Whitten [22]

$$\begin{aligned} r_x^k &= \rho\cos\Theta\cos\Phi_k,\\ r_y^k &= -\rho\sin\Theta\sin\Phi_k,\\ r_z^k &= 0\\ R_x^k &= \rho\cos\Theta\sin\Phi_k,\\ R_y^k &= \rho\sin\Theta\cos\Phi_k,\\ R_z^k &= 0, \end{aligned} \tag{B.9}$$

where Φ_k is in the range $0 \le \Phi_k < 2\pi$ and Θ is in the range $0 \le \Theta \le \pi/4$. The distances between the particles ij are related through

$$r_{ij} = |\mathbf{x}_j - \mathbf{x}_i| = d_k|\mathbf{r}_k| = \frac{d_k\rho}{2^{1/2}}\big[1 + \cos(2\Theta)\cos(2\Phi_k)\big]^{1/2}. \tag{B.10}$$

The kinematic rotations (B.8) correspond to the following transformation in hyperspherical space

$$\Phi_j = \Phi_i - \beta_{ij}. \tag{B.11}$$

This is easily shown by performing transformations within the coordinate set. If we choose $k = 3$ then

$$\begin{aligned}
r_{12} = d_3 \mid \mathbf{r}_3 \mid &= \frac{\rho d_3}{2^{1/2}}\big[1 + \cos(2\Theta)\cos(2\Phi_3)\big]^{1/2} \\
r_{23} = d_1 \mid \mathbf{r}_1 \mid &= d_1\big[\cos^2\beta_{31}\mathbf{r}_3^2 + \sin^2\beta_{31}\mathbf{R}_3^2 + 2\sin\beta_{31}\cos\beta_{31}\mathbf{r}_3\cdot\mathbf{R}_3\big]^{1/2} \\
&= \frac{d_1\rho}{2^{1/2}}\big[\cos^2\beta_{31}(1 + \cos(2\Theta)\cos(2\Phi_3)) \\
&\quad + \sin^2\beta_{31}(1 - \cos(2\Theta)\cos(2\Phi_3)) \\
&\quad + 2\sin\beta_{31}\cos\beta_{31}\cos(2\Theta)\sin(2\Phi_3)\big]^{1/2} \\
&= \frac{d_1\rho}{2^{1/2}}\big[1 + \cos(2\Theta)\big(\cos(\Phi_3)\cos(2\beta_{31}) + \sin(2\Phi_3)\sin(2\beta_{31})\big)\big]^{1/2} \\
&= \frac{d_1\rho}{2^{1/2}}\big[1 + \cos(2\Theta)\cos(2\Phi_3 - 2\beta_{31})\big]^{1/2} \\
&= \frac{d_1\rho}{2^{1/2}}\big[1 + \cos(2\Theta)\cos(2\Phi_1)\big]^{1/2} \\
r_{31} = d_2 \mid \mathbf{r}_2 \mid &= d_2\big[\cos^2\beta_{23}\mathbf{r}_3^2 + \sin^2\beta_{23}\mathbf{R}_3^2 - 2\sin\beta_{23}\cos\beta_{23}\mathbf{r}_3\cdot\mathbf{R}_3\big]^{1/2} \\
&= \frac{d_2\rho}{2^{1/2}}\big[1 + \cos(2\Theta)\big(\cos(\Phi_3)\cos(2\beta_{23}) - \sin(2\Phi_3)\sin(2\beta_{23})\big)\big]^{1/2} \\
&= \frac{d_2\rho}{2^{1/2}}\big[1 + \cos(2\Theta)\cos(2\Phi_3 + 2\beta_{23})\big]^{1/2} \\
&= \frac{d_2\rho}{2^{1/2}}\big[1 + \cos(2\Theta)\cos(2\Phi_2)\big]^{1/2}.
\end{aligned} \tag{B.12}$$

By defining

$$\begin{aligned}
\epsilon_1 &= -2\tan^{-1}(-m_2/\mu) \\
\epsilon_2 &= 2\tan^{-1}(-m_1/\mu).
\end{aligned} \tag{B.13}$$

These the distances are given by

$$\begin{aligned} r_{12} &= \frac{d_3\rho}{2^{1/2}}\left[1+\cos(2\Theta)\cos(2\Phi)\right]^{1/2} \\ r_{23} &= \frac{d_1\rho}{2^{1/2}}\left[1+\cos(2\Theta)\cos(2\Phi+\epsilon_1)\right]^{1/2} \\ r_{31} &= \frac{d_2\rho}{2^{1/2}}\left[1+\cos(2\Theta)\cos(2\Phi+\epsilon_2)\right]^{1/2} \end{aligned} \tag{B.14}$$

where the angular indice 3 is surpressed.

Kuppermann pointed out that there are some disadvantages with this representation [16]. For the mapping of the triatomic potential energy surface to configuration space, we require that every internal configuration corresponds to one point only and that a transformation of Φ_k and Θ should rotate, but not distort, the equipotential surface about the z-axis. Because each particle arrangement corresponds to two points in the hyperspherical coordinate space within the range of the hyperangles, we perform a second mapping

$$\begin{aligned} \theta &= \pi/2 - 2\Theta, \\ \tilde{\phi}_k &= \pi/2 - 2\Phi_k, \end{aligned} \tag{B.15}$$

where the ranges of these new coordinates are

$$\begin{aligned} 0 \le \theta &\le \pi/2, \\ -7\pi/2 \le \tilde{\phi}_k &< \pi/2, \end{aligned} \tag{B.16}$$

and the distances are subsequently given by

$$r_{ij} = \frac{d_k\rho}{2^{1/2}}\left[1+\sin\theta\sin\tilde{\phi}_k\right]^{1/2}. \tag{B.17}$$

To get a more conveinient range we redefine $\phi_k = \tilde{\phi}_k + 7\pi/2$, so that the range is $0 \le \phi_k < 4\pi$. Then we finally get

$$r_{ij} = \frac{d_k\rho}{2^{1/2}}\left[1+\sin\theta\cos\phi_k\right]^{1/2}, \tag{B.18}$$

where the corresponding kinetic rotations are $\phi_j = \phi_i - 2\eta_{ij}$, in which the angle η_{ij} ($2\eta_{ij} = -2\beta_{ij}$) is in the range $0 \le \eta_{ij} \le \pi/2$ and have the properties

$$\eta_{ij} = -\eta_{ji}, \quad \eta_{ii} = 0, \tag{B.19a}$$

$$\tan\eta_{ij} = m_k/\mu, \tag{B.19b}$$

$$\eta_{12} + \eta_{23} + \eta_{31} = \pi. \tag{B.19c}$$

If the cartesian coordinates of this point in configuration space is defined to be the regular spherical polar coordinates, then all configurations will map to the upper half-space $z \ge 0$ (since $z_k = \rho\cos\theta$ and $0 \le \theta \le \pi/2$). Since

ϕ_k and $\phi_k + 2\pi$ represent the same internal configuration and also points to the same point in configuration space, each point in the upper half-space represent a unique arrangement of the three-body system. Exchanging two of the particles will generate a new arrangement, which coorseponds to a new point in configuration space.

We can choose one of the branches of ϕ_k by restricting the range to $0 \leq \phi_k < 2\pi$. Finally, we choose the Jacobi coordinates where $k = 3$ and subsequently get the expression for our hyperspherical coordinates

$$\begin{aligned} r_{12} &= \frac{d_3\rho}{2^{1/2}}\left[1 + \sin\theta\cos\phi\right]^{1/2} \\ r_{23} &= \frac{d_1\rho}{2^{1/2}}\left[1 + \sin\theta\cos(\phi - \varphi_1)\right]^{1/2} \\ r_{31} &= \frac{d_2\rho}{2^{1/2}}\left[1 + \sin\theta\cos(\phi + \varphi_2)\right]^{1/2}, \end{aligned} \tag{B.20}$$

in which

$$\begin{aligned} \varphi_1 &= 2\tan^{-1}(m_2/\mu), \\ \varphi_2 &= 2\tan^{-1}(m_1/\mu). \end{aligned} \tag{B.21}$$

In fig. B.1 the triatomic potential energy surface for the model potential used in section 4.2, see eqs. (4.33) and (4.34), is shown for three identical particles. As seen in the figure, the translation and reflection symmetries reduce the range of ϕ once more to $0 \leq \phi < \pi/3$ for identical particles.

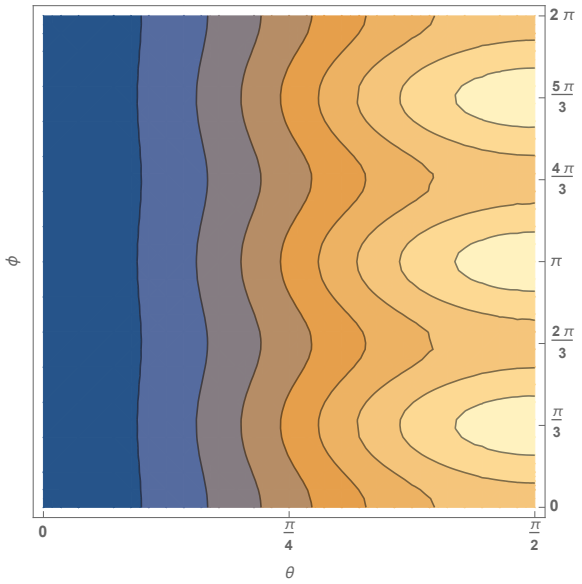

Figure B.1: Potential surface for three identical particles. Symmetries due to translations and reflections are seen at $\phi = n\pi/3,\ (n = 1 - 5)$.

B.2 Transformation of the Kinetic Energy Operator

The kinetic energy operator of a particle with mass μ in a curvilinear coordinate system of N dimensions is given by [18]

$$T = -\frac{1}{2\mu}\sum_{i=1}^{N}\sum_{j=1}^{N}\frac{1}{\sqrt{g}}\frac{\partial}{\partial q_i}\left(\sqrt{g}g^{ij}\frac{\partial}{\partial q_j}\right), \tag{B.22}$$

where g^{ij} is the inverse, or contravariant, metric tensor and g is the determinant of the covariant metric tensor $g = \det(g_{ij}) \neq 0$. The metric tensor g_{ij} describes the relationship between the set of curvilinear coordinates $\mathbf{q}$ and the set of regular Cartesian coordinates $\mathbf{x}$ through

$$g_{ij} = \sum_{\lambda=1}^{N}\frac{\partial x_\lambda}{\partial q_i}\frac{\partial x_\lambda}{\partial q_j}, \tag{B.23}$$

where $x_\lambda = x_\lambda(q_1, \ldots, q_N)$. The metric is usefull for generalizing the concept of distance to general curvilinear coordinate frames and hence maintain the invariance of distance in different coordinate systems. Invariance of the square of the line element ds^2 under coordinate transformations can also be considered to define the metric itself since

$$ds^2 = d\mathbf{x}\cdot d\mathbf{x} = \sum_{i,j}^{N} g_{ij}dq_i dq_j = g. \tag{B.24}$$

Here the displacement differential vector is given by

$$d\mathbf{x} = \frac{\partial \mathbf{x}}{\partial q_i}dq_i, \tag{B.25}$$

where $\mathbf{x}$ is the position vector.

The tranformation of interest for us is that from the mass weighted Jacobi coordinates $\mathbf{r}_k$ and $\mathbf{R}_k$ to a set of symmetric coordinates. Here we choose to work with one of the pair of the Jacobi coordinate sets $(i, j, k) = (1, 2, 3)$ and surpress the subscript 3. Since the three-body system has $N = 6$ dimensions after separating out the center-of-mass we collect the Cartesian components of the mass-weighted Jacobian vectors into the 6-position

$$\mathbf{x} = \begin{pmatrix}\mathbf{r}\\ \mathbf{R}\end{pmatrix} = \begin{pmatrix} r_x\\ r_y\\ r_z\\ R_x\\ R_y\\ R_z\end{pmatrix}. \tag{B.26}$$

At any instant, three particles form a plane in $\mathbb{R}^3$. If we consider this plane to be the xy-plane – and define the internal motion of the particles within this plane in terms of hyperspherical coordinates (ρ, Θ, Φ) – our coordinate system must rotate in this plane. That is, we use a body-fixed axis system xyz, which rotates with respect to the space-fixed axis system $x'y'z'$. The orientation of the body-fixed frame is related to the space-fixed frame by the Euler angles. With the z-axis perpendicular to the plane and with the positive axis in the direction of the vector $\mathbf{r} \times \mathbf{R}$, Smith and Whitten [22] defined these as

$$\begin{aligned} r_x &= \rho \cos\Theta \cos\Phi, \\ r_y &= -\rho \sin\Theta \sin\Phi, \\ r_z &= 0 \\ R_x &= \rho \cos\Theta \sin\Phi, \\ R_y &= \rho \sin\Theta \cos\Phi, \\ R_z &= 0. \end{aligned} \tag{B.27}$$

To describe how rotations of the body-fixed frame affects the derivatives in the space-fixed frame it is enough to consider infinitesimal rotations. Let $d\boldsymbol{\Omega}$ be the angular displacement differential vector of the rotating axes xyz with respect to the fixed axes $x'y'z'$

$$d\boldsymbol{\Omega} = \begin{pmatrix} d\Omega_x \\ d\Omega_y \\ d\Omega_z \end{pmatrix}. \tag{B.28}$$

Then the displacement differential vectors in the space-fixed frame transform like

$$d\mathbf{r}' = d\mathbf{r} + d\boldsymbol{\Omega} \times \mathbf{r}, \tag{B.29a}$$
$$d\mathbf{R}' = d\mathbf{R} + d\boldsymbol{\Omega} \times \mathbf{R}, \tag{B.29b}$$

which is given explicitly by

$$\begin{pmatrix} dr'_x \\ dr'_y \\ dr'_z \\ dR'_x \\ dR'_y \\ dR'_z \end{pmatrix} = \begin{pmatrix} \partial_\rho r_x & \partial_\Theta r_x & \partial_\Theta r_x & 0 & r_z & -r_y \\ \partial_\rho r_y & \partial_\Theta r_y & \partial_\Theta r_y & -r_z & 0 & r_x \\ \partial_\rho r_z & \partial_\Theta r_z & \partial_\Theta r_z & r_y & -r_x & 0 \\ \partial_\rho R_x & \partial_\Theta R_x & \partial_\Theta R_x & 0 & R_z & -R_y \\ \partial_\rho R_y & \partial_\Theta R_y & \partial_\Theta R_y & -R_z & 0 & R_x \\ \partial_\rho R_z & \partial_\Theta R_z & \partial_\Theta R_z & R_y & -R_x & 0 \end{pmatrix} \begin{pmatrix} d\rho \\ d\Theta \\ d\Phi \\ d\Omega_x \\ d\Omega_y \\ d\Omega_z \end{pmatrix}$$
$$= \begin{pmatrix} \mathrm{cc} & -\mathrm{sc} & -\mathrm{cs} & 0 & 0 & \mathrm{ss} \\ -\mathrm{ss} & -\mathrm{cs} & -\mathrm{sc} & 0 & 0 & \mathrm{cc} \\ 0 & 0 & 0 & -\mathrm{ss} & -\mathrm{cc} & 0 \\ \mathrm{cs} & -\mathrm{ss} & \mathrm{cc} & 0 & 0 & -\mathrm{sc} \\ \mathrm{sc} & \mathrm{cc} & -\mathrm{ss} & 0 & 0 & \mathrm{cs} \\ 0 & 0 & 0 & \mathrm{sc} & -\mathrm{cs} & 0 \end{pmatrix} \begin{pmatrix} d\rho \\ \rho d\Theta \\ \rho d\Phi \\ \rho d\Omega_x \\ \rho d\Omega_y \\ \rho d\Omega_z \end{pmatrix}, \tag{B.30}$$

where the abbreviations are $\mathrm{cc} = \cos\Theta\cos\Phi$, $\mathrm{ss} = \sin\Theta\sin\Phi$, $\mathrm{cs} = \cos\Theta\sin\Phi$ and $\mathrm{sc} = \sin\Theta\cos\Phi$. In matrix notation (B.30) may be expressed as

$$d\mathbf{x}' = \mathbf{A}d\mathbf{q}, \tag{B.31}$$

in which

$$d\mathbf{q} = \begin{pmatrix} d\rho \\ d\Theta \\ d\Phi \\ d\Omega_x \\ d\Omega_y \\ d\Omega_z \end{pmatrix}. \tag{B.32}$$

The squared line element ds^2 is then given by

$$ds^2 = d\mathbf{x}' \cdot d\mathbf{x}' = d\mathbf{q}^{\mathrm{T}}\mathbf{A}^{\mathrm{T}}\mathbf{A}d\mathbf{q} = d\mathbf{q}^{\mathrm{T}}\mathbf{g}d\mathbf{q}. \tag{B.33}$$

Here the metric tensor

$$\mathbf{g} = \begin{pmatrix} \mathbf{G} & \mathbf{C} \\ \mathbf{C}^{\mathrm{T}} & \mathbf{K} \end{pmatrix} \tag{B.34}$$

is partitioned into the submatrices $\mathbf{G}$, $\mathbf{K}$ and $\mathbf{C}$, which are given by

$$\mathbf{G} = \begin{pmatrix} 1 & 0 & 0 \\ 0 & \rho^2 & 0 \\ 0 & 0 & \rho^2 \end{pmatrix}, \tag{B.35}$$

$$\mathbf{K} = \rho^2 \begin{pmatrix} \sin^2\Theta & 0 & 0 \\ 0 & \cos^2\Theta & 0 \\ 0 & 0 & 1 \end{pmatrix}, \tag{B.36}$$

and

$$\mathbf{C} = -\rho^2 \sin^2(2\Theta) \begin{pmatrix} 0 & 0 & 0 \\ 0 & 0 & 0 \\ 0 & 0 & 1 \end{pmatrix}, \tag{B.37}$$

respectively. The inverse of the metric tensor $\mathbf{g}^{-1}$ is the given by

$$\mathbf{g}^{-1} = \begin{pmatrix} \mathbf{V} & \mathbf{W} \\ \mathbf{W}^{\mathrm{T}} & \mathbf{U} \end{pmatrix}, \tag{B.38}$$

where the submatrices $\mathbf{V}$, $\mathbf{W}$ and $\mathbf{U}$ are given by

$$\mathbf{V} = \begin{pmatrix} 1 & 0 & 0 \\ 0 & 1/\rho^2 & 0 \\ 0 & 0 & 1/\rho^2 \cos^2(2\Theta) \end{pmatrix}, \tag{B.39}$$

$$\mathbf{U} = \frac{1}{\rho^2} \begin{pmatrix} 1/\sin^2\Theta & 0 & 0 \\ 0 & 1/\cos^2\Theta & 0 \\ 0 & 0 & 1/\cos^2(2\Theta) \end{pmatrix}, \tag{B.40}$$

and

$$\mathbf{W} = \frac{\sin(2\Theta)}{\rho^2 \cos^2(2\Theta)} \begin{pmatrix} 0 & 0 & 0 \\ 0 & 0 & 0 \\ 0 & 0 & 1 \end{pmatrix}, \tag{B.41}$$

respectively. The determinant of the metric tensor is then

$$g = \mid \mathbf{g} \mid = \begin{vmatrix} \mathbf{G} & \mathbf{C} \\ \mathbf{C}^T & \mathbf{K} \end{vmatrix} = \begin{vmatrix} \mathbf{G} & \mathbf{C} \\ 0 & \mathbf{K} - \mathbf{C}^T\mathbf{G}^{-1}\mathbf{C} \end{vmatrix} \tag{B.42}$$

$$= \mid \mathbf{G} \mid \cdot \mid \mathbf{K} - \mathbf{C}^T\mathbf{G}^{-1}\mathbf{C} \mid = \frac{\rho^{10}}{16} \sin^2(4\Theta) \tag{B.43}$$

and subsequently the square root of the metric reads

$$\sqrt{g} = \frac{\rho^5}{4} \sin(4\Theta). \tag{B.44}$$

Now, if the momentum vector is given by

$$\mathbf{p} = i \begin{pmatrix} \partial/\partial q_1 \\ \vdots \\ \partial/\partial q_N \end{pmatrix} \tag{B.45}$$

we can express the kinetic energy operator given in (B.22) in terms of this vector and the metric

$$
\begin{aligned}
-T &= -\frac{1}{2\mu\sqrt{g}}\mathbf{p}^{\mathrm{T}}\sqrt{g}\mathbf{g}^{-1}\mathbf{p} \\
&= \frac{1}{2\mu\rho^5\sin(4\Theta)}\left[\frac{\partial}{\partial\rho}\left(\rho^5\sin(4\Theta)\frac{\partial}{\partial\rho}\right) + \frac{\partial}{\partial\Theta}\left(\rho^3\sin(4\Theta)\frac{\partial}{\partial\Theta}\right)\right. \\
&+ \frac{\partial}{\partial\Phi}\left(2\rho^3\tan(2\Theta)\frac{\partial}{\partial\Phi} + 2\tan^2(2\Theta)\cos(2\Theta)\frac{\partial}{\partial\Omega_z}\right) \\
&+ \frac{\partial}{\partial\Omega_x}\left(4\rho^3\cot(\Theta)\cos(2\Theta)\frac{\partial}{\partial\Omega_x}\right) \\
&+ \frac{\partial}{\partial\Omega_y}\left(4\rho^3\tan(2\Theta)\cos(2\Theta)\frac{\partial}{\partial\Omega_y}\right) \\
&\left.+ \frac{\partial}{\partial\Omega_z}\left(2\rho^3\tan^2(2\Theta)\frac{\partial}{\partial\Phi} + 2\rho^3\tan(2\Theta)\frac{\partial}{\partial\Omega_z}\right)\right] \\
&= \frac{1}{2\mu}\left[\frac{1}{\rho^5}\frac{\partial}{\partial\rho}\left(\rho^5\frac{\partial}{\partial\rho}\right) + \frac{1}{\rho^2\sin(4\Theta)}\frac{\partial}{\partial\Theta}\left(\sin(4\Theta)\frac{\partial}{\partial\Theta}\right)\right. \\
&+ \frac{1}{\rho^2\cos^2(2\Theta)}\frac{\partial^2}{\partial\Phi^2} + \frac{\sin(2\Theta)}{\rho^2\cos^2(2\Theta)}\frac{\partial}{\partial\Phi}\frac{\partial}{\partial\Omega_z} \\
&+ \frac{1}{\rho^2\sin^2(\Theta)}\frac{\partial^2}{\partial\Omega_x^2} + \frac{1}{\rho^2\cos^2(\Theta)}\frac{\partial^2}{\partial\Omega_y^2} + \frac{\sin(2\Theta)}{\rho^2\cos^2(2\Theta)}\frac{\partial}{\partial\Omega_z}\frac{\partial}{\partial\Phi} \\
&\left.+ \frac{1}{\rho^2\cos^2(2\Theta)}\frac{\partial^2}{\partial\Omega_z^2}\right] \\
&= \frac{1}{2\mu\rho^5}\frac{\partial}{\partial\rho}\left(\rho^5\frac{\partial}{\partial\rho}\right) + \frac{1}{2\mu\rho^2}\left[\frac{1}{\sin(4\Theta)}\frac{\partial}{\partial\Theta}\left(\sin(4\Theta)\frac{\partial}{\partial\Theta}\right)\right. \\
&\left.+ \frac{1}{\cos^2(2\Theta)}\frac{\partial^2}{\partial\Phi^2}\right] + \frac{1}{2\mu\rho^2}\left[\frac{1}{\sin^2(\Theta)}\frac{\partial^2}{\partial\Omega_x^2} + \frac{1}{\cos^2(\Theta)}\frac{\partial^2}{\partial\Omega_y^2} + \frac{1}{\cos^2(2\Theta)}\frac{\partial^2}{\partial\Omega_z^2}\right. \\
&\left.+ \frac{2\sin(2\Theta)}{\cos^2(2\Theta)}\frac{\partial}{\partial\Phi}\frac{\partial}{\partial\Omega_z}\right].
\end{aligned}
\tag{B.46}
$$

Now, as have been mentioned previously, we use the Euler angles α, β, γ to relate the body-fixed axes xyz with the space-fixed axes $x'y'z'$. Any coordinate frame that coincide with the space-fixed frame can be made to coincide with the body-fixed frame by performing a series of three basic rotations (right-handed). There are several ways for defining the Euler angles, the convention used by Johnson [13] is adopted here and the method is decribed in detail in [2]. If the line of nodes ξ are the intersection of the planes $x'y'$ and xy, then α is the angle between the y'-axis and the line of

nodes. The operational sequence are the following:

(i) First rotate the coordinates $x'y'z'$ counterclockwise through an angle α in the range $0 \leq \alpha < 2\pi$ about the z'-axis, using $\mathbf{S}_\alpha$, into the new coordinates $\bar{x}'\xi z'$.

(ii) Then rotate the coordinates $\bar{x}'\xi z'$ counterclockwise through an angle β $(0 \leq \beta \leq \pi)$ about the line of nodes, using $\mathbf{S}_\beta$, into the new coordinates $\bar{x}\xi z$.

(iii) Finally rotate the coordinates $\bar{x}\xi z$ counterclockwise by an angle γ $(0 \leq \gamma < 2\pi)$ about the z-axis (the former z'-axis) using $\mathbf{S}_\gamma$, into the body-fixed coordinates xyz.

The total rotation matrix is then the triple matrix product of the basic rotation matrices $\mathbf{S} = \mathbf{S}_\alpha \mathbf{S}_\beta \mathbf{S}_\gamma$, in which

$$\mathbf{S}_\alpha = \begin{pmatrix} \cos\alpha & \sin\alpha & 0 \\ -\sin\alpha & \cos\alpha & 0 \\ 0 & 0 & 1 \end{pmatrix}, \tag{B.47}$$

$$\mathbf{S}_\beta = \begin{pmatrix} \cos\beta & 0 & -\sin\beta \\ 0 & 1 & 0 \\ \sin\beta & 0 & \cos\beta \end{pmatrix}, \tag{B.48}$$

$$\mathbf{S}_\gamma = \begin{pmatrix} \cos\gamma & \sin\gamma & 0 \\ -\sin\gamma & \cos\gamma & 0 \\ 0 & 0 & 1 \end{pmatrix}, \tag{B.49}$$

and

$$\mathbf{S} = \begin{pmatrix} \cos\gamma\cos\beta\cos\alpha - \sin\gamma\sin\alpha & \cos\gamma\cos\beta\sin\alpha\sin\gamma\cos\alpha & -\cos\gamma\sin\beta \\ -\sin\gamma\cos\beta\cos\alpha - \cos\gamma\sin\alpha & \sin\gamma\cos\beta\sin\alpha + \cos\gamma\cos\alpha & \sin\gamma\sin\beta \\ \sin\beta\cos\alpha & \sin\beta\sin\alpha & \cos\beta \end{pmatrix}. \tag{B.50}$$

The cartesian coordinates $\mathbf{x}$ and $\mathbf{x}'$ of a point P in the two frames are thus related through

$$\mathbf{x} = \mathbf{S}\mathbf{x}'. \tag{B.51}$$

Now, the general angular displacement differential $d\mathbf{\Omega}$ can be considered as consisting of three consecutive infinitesimal rotations where $d\Omega_\alpha = d\alpha$, $d\Omega_\beta = d\beta$ and $d\Omega_\gamma = d\gamma$. The vector $d\mathbf{\Omega}$ can be obtained as the sum of three different angular displacement differential vectors; $d\mathbf{\Omega}_\alpha$ is along the space-fixed z'-axis, $d\mathbf{\Omega}_\beta$ is along the line of nodes and $d\mathbf{\Omega}_\gamma$ is along the body-fixed z-axis [10]. Since $d\mathbf{\Omega}_\alpha$ is along the z'-axis, its components are obtained by

the applying the total rotation matrix. Thus, if the total rotation matrix is written

$$\mathbf{S} = [\mathbf{S}_1 \quad \mathbf{S}_2 \quad \mathbf{S}_3], \tag{B.52}$$

then the body-fixed displacement differential angles $d\mathbf{\Omega}_\alpha$ are related to the Euler angles through

$$(\mathbf{\Omega}_\alpha)_\mathbf{x} = \mathbf{S}_3 d\alpha = \begin{pmatrix} -\sin\beta\cos\gamma \\ \sin\beta\sin\gamma \\ \cos\beta \end{pmatrix} d\alpha. \tag{B.53}$$

Next, because $d\mathbf{\Omega}_\beta$ is along the line of nodes, we only need to apply the last transformation $\mathbf{S}_\gamma$ to retreive

$$(\mathbf{\Omega}_\beta)_\mathbf{x} = \mathbf{S}_{\gamma_2} d\beta = \begin{pmatrix} \sin\gamma \\ \cos\gamma \\ 0 \end{pmatrix} d\beta. \tag{B.54}$$

No transformation is needed for $d\mathbf{\Omega}_\gamma$ since it is already directed along the body-fixed z-axis. The transformations are finally summarized into the total transformation matrix, which relates the body-fixed infinitesimal rotations to the Euler angles through

$$\begin{pmatrix} d\Omega_x \\ d\Omega_y \\ d\Omega_z \end{pmatrix} = \tilde{\mathbf{S}} \begin{pmatrix} d\alpha \\ d\beta \\ d\gamma \end{pmatrix}, \tag{B.55}$$

where

$$\tilde{\mathbf{S}} = \begin{pmatrix} -\sin\beta\cos\gamma & \sin\gamma & 0 \\ \sin\beta\sin\gamma & \cos\gamma & 0 \\ \cos\beta & 0 & 1 \end{pmatrix}. \tag{B.56}$$

Thus, a transformation of coordinates

$$d\mathbf{q} = \begin{pmatrix} d\rho \\ d\Theta \\ d\Phi \\ d\Omega_x \\ d\Omega_y \\ d\Omega_z \end{pmatrix} \longrightarrow d\mathbf{q}' = \begin{pmatrix} d\rho \\ d\Theta \\ d\Phi \\ d\alpha \\ d\beta \\ d\gamma \end{pmatrix} \tag{B.57}$$

correspond to a transformation of the metric, which is easily derived from the squared line element, where

$$ds^2 = d\mathbf{q}^{\mathrm{T}} \mathbf{g} d\mathbf{q} = (d\mathbf{q}')^{\mathrm{T}} \mathbf{g}' d\mathbf{q}'. \tag{B.58}$$

The metric thus transform as

$$\mathbf{g}' = \mathbf{B}^{\mathrm{T}}\mathbf{g}\mathbf{B}, \tag{B.59}$$

in which

$$\mathbf{B} = \begin{pmatrix} \mathbf{I} & 0 \\ 0 & \tilde{\mathbf{S}} \end{pmatrix}. \tag{B.60}$$

Subsequently, the square root of the determinant transform into

$$g'^{1/2} = (\mid \mathbf{B} \mid^2 \mid \mathbf{g} \mid)^{1/2} = (\mid \tilde{\mathbf{S}} \mid^2 \mid \mathbf{g} \mid)^{1/2} = \frac{\rho^5}{4} \sin(4\Theta) \sin\beta. \tag{B.61}$$

Since a general curvilinear coordinate system of N dimensions have a volume element

$$d^N v = g^{1/2} \prod_{i=1}^{N} dq_i, \tag{B.62}$$

the sought volume element is

$$d^6 v = g^{1/2} \prod_{i=1}^{6} dq_i = \frac{\rho^5}{4} \sin(4\Theta) \sin\beta d\rho d\Theta d\Phi d\alpha d\beta d\gamma. \tag{B.63}$$

Lastly, to produce a representation of the entire internal configuration space that is unbiased by the particular choice of the three Jacobi coordinate sets, we follow Kuppermann's mapping procedure [16] and make the following modification of the internal angles

$$\begin{aligned} \Theta = \frac{\pi}{4} - \frac{\theta}{2} &\implies \frac{\partial}{\partial\Theta} = -2\frac{\partial}{\partial\theta}, \\ \Phi = \frac{\pi}{4} - \frac{\phi}{2} &\implies \frac{\partial}{\partial\Phi} = -2\frac{\partial}{\partial\phi}. \end{aligned} \tag{B.64}$$

Now, define

$$\mathbf{P} = -i \begin{pmatrix} \partial/\partial\rho \\ \partial/\partial\theta \\ \partial/\partial\phi \end{pmatrix} = \begin{pmatrix} P_\rho \\ P_\theta \\ P_\phi \end{pmatrix} \tag{B.65}$$

and

$$\mathbf{J} = -i \begin{pmatrix} \partial/\partial\Omega_x \\ \partial/\partial\Omega_y \\ \partial/\partial\Omega_z \end{pmatrix} = \begin{pmatrix} J_x \\ J_y \\ J_z \end{pmatrix}, \tag{B.66}$$

where the operators J_x, J_y , and J_z are the total angular momentum operators in the body-fixed frame, which can be expressed in terms of the Euler angle coordinates by the relation

$$\begin{pmatrix} J_x \\ J_y \\ J_z \end{pmatrix} = \begin{pmatrix} -\cos\gamma/\sin\beta & \sin\gamma & \cot\beta\cos\gamma \\ \sin\gamma/\sin\beta & \cos\gamma & -\cot\beta\sin\gamma \\ 0 & 0 & 1 \end{pmatrix} \begin{pmatrix} P_\alpha \\ P_\beta \\ P_\gamma \end{pmatrix}. \tag{B.67}$$

This can be shown using the chain rule for partial differentiation

$$P_\sigma = \sum_\lambda \frac{\partial \Omega_\lambda}{\partial \sigma} J_\lambda, \tag{B.68}$$

where $\sigma = (\alpha, \beta, \gamma)$ and $\lambda = (x, y, z)$. The partial derivatives are calculated using the inverse of (B.69)

$$\tilde{\mathbf{S}}^{-1} = \begin{pmatrix} -\cos\gamma/\sin\beta & \sin\gamma/\sin\beta & 0 \\ \sin\gamma & \cos\gamma & 0 \\ \cot\beta\cos\gamma & -\cot\beta\sin\gamma & 1 \end{pmatrix}. \tag{B.69}$$

Now, using the relations

$$\begin{aligned} \sin 4\Theta &= \sin 2\theta \\ \cos^2 2\Theta &= \sin^2\theta \\ \sin^2 2\Theta &= \cos^2\theta \\ \cos^2\Theta &= \frac{1}{2}(1+\sin\theta) \\ \sin^2\Theta &= \frac{1}{2}(1-\sin\theta) \end{aligned} \tag{B.70}$$

in conjunction with (B.66) the kinetic energy operator (B.46) becomes

$$\begin{aligned} T = -\frac{\hbar^2}{2\mu}\Bigg[\frac{1}{\rho^5}\frac{\partial}{\partial\rho}\rho^5\frac{\partial}{\partial\rho} + \frac{4}{\rho^2}\Bigg(\frac{1}{\sin(2\theta)}\frac{\partial}{\partial\theta}\sin(2\theta)\frac{\partial}{\partial\theta} \\ + \frac{1}{\sin^2(\theta)}\frac{\partial^2}{\partial\phi^2}\Bigg)\Bigg] - \frac{1}{\mu\rho^2}\left[\frac{J_x^2}{(1-\sin\theta)} + \frac{J_y^2}{(1+\sin\theta)} + \frac{J_z^2}{2\sin^2\theta}\right] \\ + \frac{4i\hbar\cos\theta J_z}{2\mu\rho^2\sin^2\theta}\frac{\partial}{\partial\phi}, \end{aligned} \tag{B.71}$$

with the corresponding volume element

$$d^6v = \frac{1}{8}\rho^5\sin\theta\cos\theta\sin\beta d\rho d\theta d\phi d\alpha d\beta d\gamma. \tag{B.72}$$

If we only consider $J = 0$ states, the Hamiltonian reduces to

$$H_0 = -\frac{1}{2\mu}\left[\frac{1}{\rho^5}\frac{\partial}{\partial\rho}\rho^5\frac{\partial}{\partial\rho} + \frac{4}{\rho^2}\Big(\frac{1}{\sin(2\theta)}\frac{\partial}{\partial\theta}\sin(2\theta)\frac{\partial}{\partial\theta} + \frac{1}{\sin^2(\theta)}\frac{\partial^2}{\partial\phi^2}\Big)\right] + V(\rho,\theta,\phi). \tag{B.73}$$

By rescaling the wave function $\psi = \rho^{5/2}\Psi$ the Schrödinger equation becomes

$$H\psi = E\psi, \tag{B.74}$$

where the transformed Hamiltonian operator is given by

$$H = \rho^{5/2} H_0 \rho^{-5/2}. \tag{B.75}$$

This transformation removes the first derivative in the hyper radial kinetic-energy operator and we get the final expression for the Hamiltonian

$$H = -\frac{\hbar^2}{2\mu}\left[-\frac{15}{4}\frac{1}{\rho^2} + \frac{\partial^2}{\partial\rho^2} + \frac{4}{\rho^2}\Big(\frac{1}{\sin(2\theta)}\frac{\partial}{\partial\theta}\sin(2\theta)\frac{\partial}{\partial\theta} + \frac{1}{\sin^2(\theta)}\frac{\partial^2}{\partial\phi^2}\Big)\right] + V(\rho,\theta,\phi) \tag{B.76}$$

$$= -\frac{\hbar^2}{2\mu\rho^2}\frac{\partial^2}{\partial\rho^2} + \frac{\hbar^2}{2\mu\rho^2}\left(\Lambda^2 + \frac{15}{4}\right) + V(\rho,\theta,\phi), \tag{B.77}$$

where Λ^2 is the grand angular momentum operator.

B.3 Symmetries

The Smith-Whitten coordinates θ and ϕ are connected to the geometry of the triangle formed by the three particles. If the three particles represent the vertecis of a triangle, θ will determine its shape, while ϕ determines the arrangement of the particles at its vertecis. Now lets determine the eigenvalues and eigenfunctions of the grand angular momentum operator. For the ϕ equation we have

$$\frac{\partial^2}{\partial\phi^2}\mathrm{e}^{i\nu\phi} = -\nu^2\mathrm{e}^{i\nu\phi}, \tag{B.78}$$

so the total eigenfunction can be written

$$f_{\nu n}(\theta,\phi) = g_{n\nu}(\theta)\mathrm{e}^{i\nu\phi}. \tag{B.79}$$

For a general system we have the symmetry

$$f_{\nu n}(\theta,\phi=0) = \Pi f_{\nu n}(\theta,\phi=2\pi), \qquad \text{for} \qquad \Pi = \pm 1, \tag{B.80}$$

the symmetry of a three identical particle system will reduce the interval of ϕ to $[0, 2\pi/3]$. (symmetry group C_{3v} with irreducible representations A_1, A_2, and E), we will consider bosons and states with $J = 0$ so this leads to vibrational wave functions of A_1 symmetry and this will reduce the interval of ϕ further to $[0, \pi/3]$, so

$$f_{\nu n}(\theta, \phi = 0) = \Pi f_{\nu n}(\theta, \phi = 2\pi/3), \qquad \text{for} \qquad \Pi = \pm 1, \tag{B.81}$$

where the parity $\Pi = 1$ for bosons. Thus

$$\mathrm{e}^{i\nu 2\pi/3} = 1 \quad \Leftrightarrow \quad \nu = 3n \quad \text{for} \quad n = 0, 1, 2, ... \tag{B.82}$$

so we get

$$\Lambda^2 g_{n\nu}(\theta) = -4\left(\frac{1}{\sin(2\theta)} \frac{\partial}{\partial\theta} \sin(2\theta) \frac{\partial}{\partial\theta} - \frac{\nu^2}{\sin^2(\theta)} \right) g_{n\nu}(\theta) = \lambda_{n\nu} g_{n\nu}(\theta). \tag{B.83}$$

The interval for θ is $[0, \pi/2]$. Lets look at the boundary as $\theta \to 0$. The small angle approximation leads to

$$\Lambda^2 \to -4\left(\frac{1}{\theta} \frac{\partial}{\partial\theta} + \frac{\partial^2}{\partial\theta^2} - \frac{\nu^2}{\theta^2} \right) g_{n\nu}(\theta) = \lambda_{n\nu} g_{n\nu}(\theta). \tag{B.84}$$

we thus need to solve a differential equation of the form

$$g''_{n\nu}(\theta) + \frac{P(\theta)}{\theta} g'_{n\nu}(\theta) + \frac{Q(\theta)}{\theta^2} g_{n\nu}(\theta) = 0, \tag{B.85}$$

with

$$P(\theta) = 1 \quad \text{and} \quad Q(\theta) = \frac{\lambda_{n\nu}\theta^2 - 4\nu^2}{4}. \tag{B.86}$$

Since ref[the differential equation] has a regular singular point at $\theta = 0$ and both $P(\theta)$ and $Q(\theta)$ are analytic functions, we seek a power series solution of the form

$$g_{n\nu}(\theta) = \sum_{k=0}^{\infty} A_k \theta^{k+s}, \quad (A_0 \neq 0). \tag{B.87}$$

differentiating

$$g'_{n\nu}(\theta) = \sum_{k=0}^{\infty} (k+s) A_k \theta^{k+s-1}, \tag{B.88}$$

$$g''_{n\nu}(\theta) = \sum_{k=0}^{\infty} (k+s)(k+s-1) A_k \theta^{k+s-2}, \tag{B.89}$$

and substituting into [ref] we get

$$\sum_{k=0}^{\infty}\left((k+s)(k+s-1)+(k+s)-\nu^2\right)A_k\theta^{k+s-2}+\left(\frac{\lambda_{n\nu}}{4}\right)A_k\theta^{k+s}=$$
$$\left[s(s-1)+s-\nu^2\right]A_0\theta^{s-2}+\sum_{k=1}^{\infty}\left(\left[(k+s)(k+s-1)+(k+s)-\nu^2\right]A_k+\frac{\lambda_{n\nu}}{4}A_{k-2}\right)\theta^{k+s-2}$$

From $s^2-\nu^2=0$ we get the two roots $s=\pm\nu$. Using these roots, we set the coefficients of θ^{k+s-2} to be zero, and we get the equations

$$\left(k^2\pm 2k\nu\right)A_k=\frac{\lambda_{n\nu}}{4}A_{k-2} \tag{B.90}$$

The table B.1 shows the analytically derived eigenvalues in SW-coordinates.

$\nu=0$	$\nu=3$	$\nu=6$	Total	$\lambda(\lambda+4)$	multiplicity
0	60	192	0	0	1
32	140	320	32	4	1
96	252	480	60	6	1
192	396	672	96	8	1
320	572	896	140	10	1
480	780	1152	192	12	2
672	1020	1440	252	14	1

Table B.1: Analytically derived eigenvalues

Appendix C

Basis Splines

A basis spline, or B-spline, of order k is a piecewise polynomial function of degree $(k-1)$ defined on a collection of points, t_i, called *knot points*. The array formed by these knot points are refered to as *knot sequence*, or knot vector, where $t_i \leq t_{i+1}$. B-splines of order k can be defined recursively by the Cox-de Boor formula. With a given knot sequence, the B-splines of order $k = 1$ is defined as

$$B_{i,k=1}(x) \doteq \begin{cases} 1, & \text{if} \quad t_i \leq x < t_{i+1} \\ 0, & \text{otherwise} \end{cases} \tag{C.1}$$

and if $k > 1$

$$B_{i,k}(x) \doteq \frac{x - t_i}{t_{i+k-1} - t_i} B_{i,k-1}(x) + \frac{t_{i+k} - x}{t_{i+k} - t_{i+1}} B_{i+1,k-1}(x). \tag{C.2}$$

The B-splines are local in the sense that they will be non-zero only in a limited region of space. If the numbering is such that the first knot point is t_1 and the first B-spline is $B_{1,k}$, then the B-spline $B_{i,k}$ is non-zero within the region $t_i \leq x \leq t_{i+k}$. On a given knot sequence $(t_1, \ldots, t_P)$ the B-splines form a complete set

$$\sum_{i=1}^{P} B_{i,k}(x) = 1. \tag{C.3}$$

By placing $(k-1)$ additional points, called ghost points, at the end-points, the B-splines will be confined within the region $t_1 \leq x \leq t_P$. This means that P knot points correspond to $N = P - 2(k-1)$ physical points. B-splines of orders $k = 1 - 4$ are shown in fig. C.1. The first derivative of a B-spline of order k is given by

$$\frac{\partial}{\partial x} B_{i,k}(x) = (k-1)\left(\frac{B_{i,k-1}(x)}{t_{i+k-1} - t_i} + \frac{B_{i+1,k-1}(x)}{t_{i+k} - t_{i+1}} \right), \tag{C.4}$$

and the second derivative

$$\frac{\partial^2}{\partial x^2}B_{i,k}(x) = \frac{(k-1)(k-2)B_{i,k-2}(x)}{(t_{i+k-1}-t_i)(t_{i+k-2}-t_i)} - \frac{(k-1)(k-2)B_{i+1,k-2}(x)}{(t_{i+k-1}-t_i)(t_{i+k-1}-t_{i+1})} - \frac{(k-1)(k-2)B_{i+1,k-2}(x)}{(t_{i+k}-t_{i+1})(t_{i+k-1}-t_{i+1})} + \frac{(k-1)(k-2)B_{i+2,k-2}(x)}{(t_{i+k}-t_{i+1})(t_{i+k}-t_{i+2})}. \tag{C.5}$$

The approach of placing the ghost points in the end-points is common because at the first physical point only the first B-spline non-zero and only the first two B-splines will have non-zero derivatives. Likewise, at the last physical point only the last B-spline will be non-zero and only the two last B-splines will have non-zero derivatives. Consequently, this choice favors implementation of boundary conditions which require the function or it's derivative to be zero at the boundary.

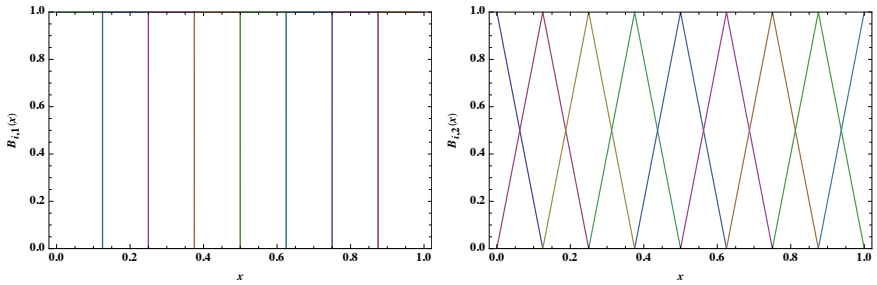

(a) $k = 1$

(b) $k = 2$

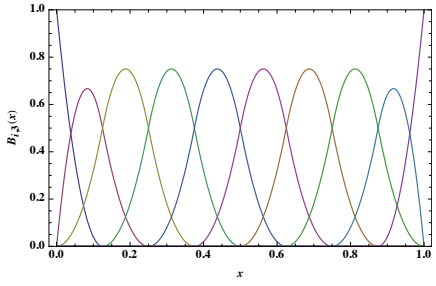

(c) $k = 3$

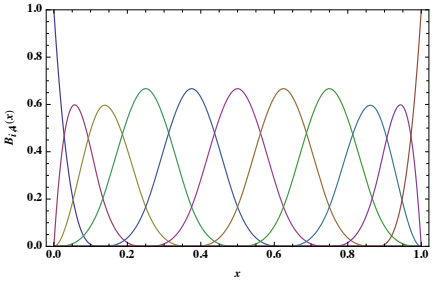

(d) $k = 4$

Figure C.1: The subfigures above show the B-splines $B_{i,k}(x)$ of different orders k on a one dimensional mesh.

Bibliography

[1] *Advances In Atomic, Molecular, and Optical Physics*. URL: https://www.sciencedirect.com/bookseries/advances-in-atomic-molecular-and-optical-physics/vol/62/suppl/C.

[2] George B. Arfken, Hans J. Weber, and Frank E. Harris. *Mathematical methods for physicists a comprehensive guide*. 7th ed. Elsevier, 2013.

[3] Kajsa-My Blomdahl. "Numerical Calculations of Efimov States in Ultracold Atomic Systems". MA thesis. http://www.diva-portal.org: KTH, 2016.

[4] Eric Braaten, Masaoki Kusunoki, and Dongqing Zhang. "Scattering models for ultracold atoms". In: *Annals of Physics* 323 (July 2008), pp. 1770–1815. DOI: 10.1016/j.aop.2007.12.004. arXiv: 0709.0499 [cond-mat.other].

[5] Alain Chenciner. "Poincaré and the Three-Body Problem". In: *Henri Poincaré, 1912–2012: Poincaré Seminar 2012*. Ed. by Bertrand Duplantier and Vincent Rivasseau. Basel: Springer Basel, 2015, pp. 51–149. ISBN: 978-3-0348-0834-7. DOI: 10.1007/978-3-0348-0834-7_2. URL: https://doi.org/10.1007/978-3-0348-0834-7_2.

[6] V. Efimov. "Energy levels arising form the resonant two-body forces in a three-body system". In: *Phys. Lett.* 33B (1970), pp. 563–564. DOI: 10.1016/0370-2693(70)90349-7.

[7] Vitaly Efimov. "Is a qualitative approach to the three-body problem useful?" In: *Comments Nucl. Part. Phys.* 19 (1990), pp. 271–293.

[8] L. D. Faddeev. "Scattering theory for a three particle system". In: *Sov. Phys. JETP* 12 (1961). [Zh. Eksp. Teor. Fiz.39,1459(1960)], pp. 1014–1019.

[9] Francesca Ferlaino et al. "Evidence for Universal Four-Body States Tied to an Efimov Trimer". In: *Physical review letters* 102 (May 2009), p. 140401. DOI: 10.1103/PHYSREVLETT.102.140401.

[10] Herbert Goldstein, Charles Poole, and John Safko. *Classical mechanics*. Addison Wesley, 2000. URL: https://detritus.fundacioace.com/pub/books/Classical_Mechanics_Goldstein_3ed.pdf.

[11] Bo Huang et al. "Observation of the Second Triatomic Resonance in Efimov's Scenario". In: *Phys. Rev. Lett.* 112 (19 May 2014), p. 190401. DOI: 10.1103/PhysRevLett.112.190401. URL: https://link.aps.org/doi/10.1103/PhysRevLett.112.190401.

[12] B. R. Johnson. "On hyperspherical coordinates and mapping the internal configurations of a three body system". In: *The Journal of Chemical Physics* 73.10 (1980), pp. 5051–5058. DOI: 10.1063/1.439983. eprint: https://doi.org/10.1063/1.439983. URL: https://doi.org/10.1063/1.439983.

[13] B. R. Johnson. "The classical dynamics of three particles in hyperspherical coordinates". In: *The Journal of Chemical Physics* 79.4 (1983), pp. 1906–1915. DOI: 10.1063/1.445969. eprint: https://doi.org/10.1063/1.445969. URL: https://doi.org/10.1063/1.445969.

[14] T. Kraemer et al. "Evidence for Efimov quantum states in an ultracold gas of caesium atoms". In: *Nature* 440 (Mar. 2006), URL: http://dx.doi.org/10.1038/nature04626.

[15] Maksim Kunitski et al. "Observation of the Efimov state of the helium trimer". In: *Science* 348 (2015), pp. 551–555. DOI: 10.1126/science.aaa5601. arXiv: 1512.02036 [physics.atm-clus].

[16] Aron Kuppermann. "A useful mapping of triatomic potential energy surfaces". In: *Chemical Physics Letters* 32.2 (1975), pp. 374–375. ISSN: 0009-2614. DOI: https://doi.org/10.1016/0009-2614(75)85148-7. URL: http://www.sciencedirect.com/science/article/pii/0009261475851487.

[17] L. D. Landau and L. M. Lifshitz. *Quantum Mechanics Non-Relativistic Theory, Second Edition: Volume 3*. 2nd ed. Pergamon Press, 1965. ISBN: 0750635398.

[18] Boris Podolsky. "Quantum-Mechanically Correct Form of Hamiltonian Function for Conservative Systems". In: *Physical Review* 32.5 (1928), pp. 812–816. DOI: 10.1103/physrev.32.812.

[19] H R Sadeghpour et al. "Collisions near threshold in atomic and molecular physics". In: *Journal of Physics B: Atomic, Molecular and Optical Physics* 33.5 (Feb. 2000), R93–R140. DOI: 10.1088/0953-4075/33/5/201. URL: https://www.cfa.harvard.edu/~hrs/PubList/JPBThresholdReviw2000.pdhttps://doi.org/10.1088%2F0953-4075%2F33%2F5%2F201.

[20] Cristina Sanz-Sanz et al. "Non-adiabatic couplings and dynamics in proton transfer reactions of Hn+ systems: Application to H2+H2+ → H+H3+ collisions". In: *The Journal of Chemical Physics* 143.23 (2015), p. 234303. DOI: 10.1063/1.4937138. eprint: https://doi.

org/10.1063/1.4937138. URL: https://doi.org/10.1063/1.4937138.

[21] Felix T. Smith. "A Symmetric Representation for Three Body Problems. I. Motion in a Plane". In: *Journal of Mathematical Physics* 3.4 (1962), pp. 735–748. DOI: 10.1063/1.1724275. eprint: https://doi.org/10.1063/1.1724275. URL: https://doi.org/10.1063/1.1724275.

[22] R. C. Whitten and F. T. Smith. "Symmetric Representation for Three-Body Problems. II. Motion in Space". In: *Journal of Mathematical Physics* 9.7 (1968), pp. 1103–1113. DOI: 10.1063/1.1664683. eprint: https://doi.org/10.1063/1.1664683. URL: https://doi.org/10.1063/1.1664683.

[23] Alexander L. Zubarev and Victor B. Mandelzweig. "Exact solution of the four-body Faddeev-Yakubovsky equations for the harmonic oscillator". In: *Phys. Rev. C* 50 (1 July 1994), pp. 38–47. DOI: 10.1103/PhysRevC.50.38. URL: https://link.aps.org/doi/10.1103/PhysRevC.50.38.